

24 **Abstract**

25

26 The molecular pathogenesis of diabetes is multifactorial, involving genetic predisposition and
27 environmental factors that are not yet fully understood. However, pancreatic β -cell failure remains
28 among the primary reasons underlying the progression of type-2 diabetes (T2D) making targeting β -cell
29 dysfunction an attractive pathway for diabetes treatment. To identify genetic contributors to β -cell
30 dysfunction, we investigated single-cell gene expression changes in β -cells from healthy (C57BL/6J)
31 and diabetic (NZO/HILtJ) mice fed with normal or high-fat, high-sugar diet (HFHS). Our study presents
32 an innovative integration of the causal network perturbation assessment (ssNPA) framework with meta-
33 cell transcriptome analysis to explore the genetic underpinnings of type-2 diabetes (T2D). By
34 generating a reference causal network and *in silico* perturbation, we identified novel genes implicated in
35 T2D and validated our candidates using the Knockout Mouse Phenotyping (KOMP) Project database.

36 Introduction

37 Type 2 diabetes (T2D) comprises more than 90% of all diabetes cases, impacting approximately 6.8%
38 (537 million individuals) of the global population in the year 2021 (Zheng et al., 2018; Sun et al., 2022).
39 T2D is a multifactorial disease caused by a complex interplay between genetic and environmental
40 factors. However, while some of the major environmental factors (i.e., diet and physical activity) are well
41 known, the genetic bases of T2D remain poorly understood. The endocrine portion of the pancreas is
42 constituted by highly specialized hormone-secreting entities known as islets of Langerhans. The islets
43 comprise β , α , delta, PP, and ghrelin cells that secrete insulin, glucagon, somatostatin, pancreatic
44 polypeptide, and ghrelin, respectively. Islet and/or β -cell dysfunctions are central to diabetes, and the
45 onset of full-blown T2D occurs when α or β cells lose their capacity to secrete appropriate amounts of
46 insulin in response to elevated blood glucose levels. Current research on Type 2 diabetes faces
47 significant limitations due to the variability in genetic, environmental, and lifestyle factors among diverse
48 populations, which challenges the generalizability of findings. Additionally, there is a notable gap in
49 long-term clinical trials that comprehensively assess the efficacy of emerging treatments across
50 different stages of the disease. In recent years, single-cell RNA sequencing (scRNA-seq) has proven
51 critical for investigating comprehensive gene expression profiles, revealing the presence of
52 heterogeneous gene expression patterns, even within cells of the same type. Furthermore, diverse
53 phenotypes of pancreatic β cells have been observed within a single islet (Hrovatin et al., 2023,
54 Camunas-Soler et al., 2020; Bhakti et al., 2019). The application of scRNA-seq has significantly
55 contributed to our understanding of β -cell maturation, β -cell heterogeneity, β -cell failure, and β -cell
56 function in both healthy and diseased states. For this study, we used the polygenic NZO/HILtJ mouse
57 strain that displays signs of morbid obesity, fasting hyperglycemia, hyperinsulinemia, insulin resistance,
58 and hypercholesterolemia resembling human T2D (Leiter et al., 1998; Ortlepp et al., 2000; Reifsnyder et
59 al., 2002). Mice from the NZO/HILtJ strain and healthy C57BL/6J controls were kept on a standard or
60 high-fat high-sugar (HFHS) diet regimen for XY days. At the end of the treatment, we analyzed the
61 single-cell gene expression profile of β -cells derived from NZO/HILtJ mice and compared it to that of β -
62 cells from healthy C57BL/6J mice (**Figure 1A**). To explore the genetic underpinnings of T2D, it is
63 crucial to identify gene perturbations and hub genes associated with the disease. We hypothesize that
64 conventional differential gene expression analysis does not effectively detect certain type of disruptions
65 in gene networks. To overcome this limitation, we extend a causal network perturbation assessment
66 (ssNPA) framework (Buschur, Chikina, & Benos, 2020) in combination with a meta-cell transcriptome
67 analysis. This approach, termed meta-ssNPA workflow, allowed us to identify genes and gene networks
68 that are perturbed in T2D mice in response to diet changes, providing valuable insights into its genetic

69 landscape. Briefly, this study aimed to juxtapose three distinct physiological states, encompassing a
70 spectrum from health to disease conditions, specifically: 1) a comparison between healthy and
71 prediabetic states (C57BL/6J mice on a normal chow diet vs. C57BL/6J on a HFHS diet); 2) a
72 comparison between prediabetic and severely diabetic states (comparing C57BL/6J mice on a HFHS
73 diet with NZO/ShiLt mice on a HFHS diet); and 3) a comparison between mildly diabetic and severely
74 diabetic states (evaluating NZO/ShiLt mice on normal or HFHS diet conditions). We focused our
75 analysis on the transcriptional profile of pancreatic beta cells due to their pivotal role in upholding
76 glucose homeostasis and serving as the primary source of insulin.

77

78 We successfully detected novel T2D genes that is not differentially expressed and validated them with
79 Knockout Mouse Phenotyping (KOMP) Project database. The KOMP database, accessible at the
80 International Mouse Phenotyping Consortium website, serves as a valuable resource for researchers,
81 offering comprehensive phenotypic data and genetic insights on a wide array of knockout mouse
82 models. This platform facilitates the understanding of gene function and disease mechanisms and is
83 instrumental in advancing the study of human diseases, including the identification of potential
84 therapeutic targets.

85 **Material & Methods**

86

87 **Animal studies and islet isolation**

88

89 In strict adherence to the standards set by the Association for Assessment and Accreditation of
90 Laboratory Animal Care, our facility at The Jackson Laboratory has upheld the care and treatment of
91 mice. We acquired male and female mice from three distinct strains: C57BL/6J (B6;
92 RRID:IMSR_JAX:000664), and NZO/HILtJ (NZO; RRID:IMSR_JAX:002105), starting at the age of four
93 weeks. The mice were provided with two types of diets from Research Diets: a high-fat, high-sucrose
94 diet (HFHS, comprising 44% kcal from fat and 1360 kcal from sucrose; Research Diets D19070208)
95 and a control diet (10% kcal from fat and devoid of sucrose; Research Diets D19072203), both
96 containing equal fiber content. The diets were given *ad libitum* starting from the age of six weeks. At the
97 age of fifteen weeks islet isolation was performed and mice were euthanized through cervical
98 dislocation. and the common bile duct at the Sphincter of Oddi was clamped. Collagenase solution
99 (three milliliters of a solution containing collagenase P (5 units/ml) and DNaseI (1mg/ml) in Hank's
100 Balanced Salt Solution (HBSS) was inserted into the bile duct proximal to the final bifurcation leading to
101 the liver to inflate the pancreas. We then removed the pancreas for digestion at 37°C for 40 minutes.
102 Post-digestion, samples were agitated for ten seconds, diluted it with 10 ml of HBSS, and centrifuged
103 for 3 minutes at 300 RPM. After two washes with HBSS, the pellet was resuspended in 5ml HBSS, and
104 handpicked islets were collected using a clean petri dish containing HBSS. We. The islets were then
105 transferred to 24-well plates with 1ml of the warmed media (containing RPMI 1640, 10% FBS,
106 glutamine, and HEPES) and incubated overnight at 37°C. After overnight incubation islets were
107 centrifuged and the supernatant was discarded. Finally, islets were resuspended in 1-2 ml of StemPro
108 Accutase dissociation solution (A1110501, Fisher Scientific), which had been preheated to 37°C. The
109 cell suspension was gently pipetted for 30 seconds to facilitate the dissociation of islets until the media
110 appeared translucent and there were no visible clumps, usually within 2-5 minutes. Following
111 dissociation, 2-3ml of RPMI complete medium was added, and the cell suspension was filtered through
112 a 20um strainer. The cells were then centrifuged at 230 RCF for 3 minutes, the supernatant was
113 removed, and the cells were resuspended in 2-3ml of RPMI complete medium.

114

115

116 **Preprocessing of Single Cell RNA-Seq**

117

118 We processed raw fastq reads from Illumina sequencing for scRNA-Seq by aligning them to the mouse
119 reference genome (mm10/GRCm38) using 10X Cell Ranger version 6.1.1 with standard settings.

120

121 To demultiplex the strain of origin from samples containing mixed strains, we employed demuxlet
122 version 2 (<https://github.com/statgen/popscler>; (Kang et al., 2018)), utilizing known genomic variations
123 from VCF files obtained from the Sanger Mouse Genomes Project ((Keane et al., 2011)). We focused
124 on sites that were biallelic and varied among our two strains (B6, and NZO). We ran demuxlet on RNA-
125 Seq data with specific parameters “--alpha 0.0 --alpha 0.5 --tag-group CB --tag-UMI UB --field GT”,
126 accounting for all cells identified by Cell Ranger.

127

128 **Quality Control and Filtering of Single Cell RNA-Seq Data**

129

130 Post-processing, we applied quality control measures to the feature count matrices generated by Cell
131 Ranger. Single cells with fewer than 500 (islet) genes, more than 20% (islet) mitochondrial transcripts,
132 or over 50% ribosomal transcripts were excluded. Additionally, genes not detected in at least three
133 single cells per sequenced library were also omitted. To correct for potential ambient RNA
134 contamination in islet samples, we utilized decontX from the celda V1.10.0 package, adhering to
135 developer guidelines on GitHub. The SCDS V1.10.0 package was deployed to eliminate cell doublets,
136 using default settings.

137

138 **Clustering and Identification of Cell Types in Single Cell RNA-Seq**

139

140 Following the filtration and quality control, single cells/nuclei underwent normalization and were
141 clustered using Seurat version 4.1, with batch variations across libraries corrected by harmony version
142 0.1.0. Gene expression data from single cells were normalized based on library size and log-
143 transformed. Dimensionality was reduced using principal component analysis (PCA) on the 2,500 most
144 variable genes, and these principal components (PCs) underwent batch correction using harmony. The
145 batch-corrected PCs were then used for Louvain-based clustering, with the resolution parameter
146 adjusted between 0.1 and 1 according to the dataset specifics.

147

148 We identified differential marker genes for various groups via the Wilcoxon rank-sum test or MAST
149 within the Seurat package, employing an FDR cutoff of 0.1 and a fold change cutoff of 1.5. Cluster-
150 specific genes aided in assigning cell types. Independently, cell type assignment was also performed
151 unbiasedly using the SingleR package, comparing each single-cell transcriptome to reference
152 transcriptome profiles of known cell types. For formal differential gene expression tests, we created
153 pseudobulks within cell types by aggregating gene expression counts across all cells of a given type
154 from a single mouse, applying DESeq2 on the pseudobulks. This approach using negative binomial
155 modeling with pseudobulks derived from single-cell transcriptomic data is noted for its efficacy and

156 accuracy in differential expression testing in single-cell contexts (Love et al., 2014). Low-expression
157 genes have been filtered out the OGFSC algorithm (Hao, Cao, Huang, Zou, & Han, 2019).

158

159 **Refine the existing Single Sample Network Perturbation Assessment (ssNPA) method**

160 However, many limitations still exist for the existing ssNPA framework (Buschur, Chikina, & Benos,
161 2020). The first limitation is the framework doesn't work well on single cell data. The single cell data
162 have sparsity issues where a lot of genes have zero expressions in many cells. This violates the
163 assumption of linear model ssNPA is using and thus the prediction performance is bad. We tackle this
164 problem by a simple meta-cell idea (Baran, Y., Bercovich, 2019). We randomly pick several cells from
165 the same cell type and average the gene expressions as a new meta-cell sample. This approach
166 maintains the relative level of all gene expression in the cell (high expression genes are still higher and
167 lower expression genes are still lower in the meta-cells) while removing the zeros. Secondly, original
168 ssNPA use simple criterion to filter out Perturbed genes: as long as the average Perturbance Score is
169 higher in the test group than the control group, the gene is annotated as a Perturbed Gene. This
170 approach doesn't consider the random noise in the Perturbance Score, thus induces False Positive
171 results. We refined this process by applying Wilcoxon test (Li, Ge, Peng, Li, & Li, 2022) onto test and
172 control group Perturbance Score and use False Discovery Rate (fDR) < 0.05 as the threshold to filter
173 the Perturbed Genes where statistical significance is introduced in the comparison. We performed one
174 sided Wilcoxon test with alternative hypothesis: control group Perturbance Score < test group
175 Perturbance Score.

176

177 **Workflow and experimental design**

178 Based on the discussion above, we propose the following meta-ssNPA workflow (**Figure 1B, S0 and**
179 **S0'**): the single-cell RNA-seq data from various sample groups underwent standard processing using a
180 single-cell pipeline to identify distinct cell types. Subsequently, meta-cell transcriptome data was
181 generated for each of these identified cell types. Using the control group samples as a reference
182 dataset, perturbation scores were computed for all genes within a given gene network, employing the
183 ssNPA framework. Perturbance scores were calculated by comparing the network predictions derived
184 from the reference network and the test group data, with the expectation of distinguishing between the
185 test and control groups. Then, we visualize all samples perturbation score with t-sne and compare them
186 against real group ID (test or control). After verifying that the test and control group are separated well
187 in visualization indicating the Perturbance Scores can be used to distinguish the two groups. The
188 Wilcoxon tests (Li, Ge, Peng, Li, & Li, 2022) were applied to filter out genes exhibiting significant
189 perturbations, and finally, pathway analysis was conducted for further interpretation of the findings. The

190 genes with a significant adjusted p-value (< 0.05) in the Wilcoxon test between test and control
191 perturbation score is defined as Perturbed Genes.

192 **DEG analysis**

193 To identify differentially expressed genes (DEGs) associated with diet, we applied the Wilcoxon test on
194 single cell expression data between control and test group for Beta cells using the same code in (Li,
195 Ge, Peng, Li, & Li, 2022). Genes with a False Discovery Rate (fDR) < 0.05 were considered DEGs.
196 Venn diagrams were generated to visualize the overlap between perturbed genes and DEGs.

197

198 **Pathway Analysis assessment: perturbed and differentially expressed genes**

199 Gene set enrichment analysis of KEGG mouse pathways was conducted using the hypergeometric
200 test. This analysis assessed both perturbed genes and differentially expressed genes (DEGs). The
201 pathways were ranked based on their p-values, and the top 10 pathways with the lowest p-values were
202 selected.

203 Results

204 Workflow to detect perturbed genes via meta-cell local reference causal network

205 We combined a meta-cell transcriptome analysis with the ssNPA framework to identify the genes that
206 are perturbed in the test condition (High Fat High Sugar diet) compared to that of the control using a
207 causal network (Buschur, Chikina, & Benos, 2020). The causal network is computed using a Fast
208 Greedy Equivalent Search (FGES) algorithm (Ramsey, Glymour, Sanchez-Romero, & Glymour, 2017)
209 on a directed acyclic graph (DAG), where the nodes are genes, and the directed edges are the causal
210 relationships between the genes. The FGES algorithm iteratively adds an edge if the addition
211 decreases the Bayesian Information Criteria (BIC) where BIC is calculated based on a linear model
212 where the expression of a gene is predicted by fitting a linear model with the expression levels of its
213 parents, spouses, and children (Markov Blanket) in the current network as the predictors. The single-
214 cell gene expression data from the mouse given the standard diet is used to construct the causal
215 network. The difference between the predicted and actual values (i.e., perturbation score) is used to
216 identify genes essential for T2D pathogenesis. Since, unlike the standard differential expression
217 analysis, this method considers the interactions between the genes and their neighbors, several genes
218 identified in our analysis could not have been identified otherwise. Importantly, the expression level of
219 perturbed genes – quantified by differential expression analysis – can be similar between test and
220 control groups, but the interactions between them and their neighbor genes vary.

221

222 Identification of differentially expressed and perturbed genes in β cells in healthy vs prediabetic 223 state

224 To identify prediabetic-states-specific perturbed genes, we performed ssNPA analysis using single-cell
225 transcriptomes of β cells isolated from C57BL/6J mice fed on HFHS diet (test group) vs. those kept on
226 a standard (control group). Only male mice are used since female mice are observed to be more
227 resistant to T2D. The β cells exhibited differentially expressed genes (DEGs) (Wilcoxon Test) and
228 perturbed genes when comparing a normal diet to a HFHS diet. Furthermore, there were shared DEGs
229 and meta-ssNPA perturbed gene signatures. Among the highly upregulated perturbed genes were
230 *Gadd45b*, *Hmgn2*, *Cartpt*, *Hdgfl3* (**Figure 2A**). Conversely, the downregulated perturbed genes
231 included *Trim12a*, *Col27a1*, *Ly6a*, *Rflna*, and *AY036118*. We performed pathway enrichment analysis
232 using hypergeometric test for the perturbed genes. Multiple pathways enriched for perturbed genes are
233 related to T2D biology (**Figure 2B**). The MAPK signaling pathway plays a crucial role in T2D by
234 affecting insulin signaling and beta-cell function. An article in the journal Diabetes assessed the
235 increased MAPK activation and its impact on insulin signaling in microvascular endothelial cells in T2D,
236 highlighting the functional role of endothelin-1 (Gogg, Smith, & Jansson, 2009).

237 **Identification of hub genes, drivers and network analysis**

238 The meta-ssNPA analysis revealed perturbed genes strongly linked to T2D. Due the large size of the
239 network, only a sub network with non-DEG perturbed genes is shown (**Figure 2C**). A full version of the
240 network is shown in **Figure S1**. In this representation, gene names (in red) and triangles denote genes
241 that are perturbed but not differentially expressed, while those in green nodes indicate downregulated
242 perturbed genes, and red node denotes upregulated perturbed genes. The out degree of the genes (top
243 20) in the perturbed network is shown as bar plot in **Figure 2D**. The out-degree of a gene quantifies the
244 number of other genes being affected by the chosen gene. The genes with highest out-degree are:
245 *Zbtb20*, *Zdhhc2*, *Ndufa4*, *Rpl7*, and *Gnai2*. Multiple detected perturbed genes are related to T2D
246 biology. The *GLP1R* gene, which encodes the glucagon-like peptide-1 receptor, plays a crucial role in
247 modulating insulin secretion in response to blood glucose levels and has been targeted by a number of
248 antidiabetic therapies (Ussher et al., 2023; Müller et al., 2019). Similarly, the Insulin-like growth factor 1
249 receptor (IGF-1R) is a receptor tyrosine kinase that plays a significant role in mediating the effects of
250 insulin-like growth factor 1 (IGF-1) on cell growth, proliferation, and metabolism. While primarily
251 recognized for its involvement in growth and development, emerging evidence suggests its implication
252 in diabetes and related metabolic disorders and targeting IGF-1R signaling pathways may hold promise
253 as a therapeutic strategy for diabetes and its associated complications (O'Neill et al., 2015; Viana-
254 Huete et al., 2016). Another gene of interest is MAFA, a transcription factor critical for pancreatic β -cell
255 function and insulin gene regulation, which may serve as a biomarker for β -cell dysfunction in T2DM
256 (Nishimura et al., 2015). Additionally, the PYY gene, which produces peptide YY, a hormone involved
257 in appetite regulation, links obesity, a significant risk factor for T2DM, to this metabolic disorder (Tan et
258 al., 2023). Some of the genes highlighted in the network pathway are *Neurogenin3*, *Glp-1r*, *Slc30a8*,
259 *Serpinb9*, *Gabra4*, *Cacna2d2*, *Angptl4* and *Lpl*.

260 *Neurogenin3* (Neurog3) is a transcription factor pivotal in developing pancreatic endocrine cells,
261 including insulin-producing β cells. In mice, the absence of *Ngn3* results in the complete absence of
262 endocrine cells within the pancreas (Gradwohl et al., 2000). The *Cacna2d2* gene, encoding the alpha-
263 2-delta-2 subunit of voltage-gated calcium channels, have demonstrated that alterations in *Cacna2d2*
264 expression or function can impact insulin sensitivity and glucose metabolism (Huang et al., 2020;
265 Cromer et al., 2015) *Slc30a8*, also known as Zinc transporter 8 (ZnT8), has garnered significant
266 attention in the field of T2D research due to its role in insulin secretion and glucose homeostasis. This
267 gene encodes a zinc transporter protein primarily expressed in pancreatic β cells, where it plays a vital
268 role in packaging zinc into insulin-containing vesicles. Several studies have demonstrated a strong
269 association between genetic variants in *SLC30A8* and the risk of developing T2D. One of the most well-
270 known and extensively studied *SLC30A8* variants is rs13266634, located in the intron of *SLC30A8*.

271 This variant has been consistently linked to an increased risk of T2D in various populations, including
272 European, Asian, and African descent groups. Studies conducted by the groundbreaking Diabetes
273 Genetics Replication and Meta-analysis (DIAGRAM) Consortium, have identified this variant as one of
274 the key risk factors for T2D (Chimenti et al., 2006; Sladek et al., 2007; Scott et al., 2007)

275 276 **Validation of prediabetic perturbed genes using the KOMP database**

277 To corroborate the perturbed genes identified with the meta-ssNPA analysis, we employed the KOMP
278 database and generated visual representations for the genes previously linked to T2D. The in-vivo
279 mouse reference data for validation of genes was generated by the Knock-out Mouse Project-KOMP
280 (www.mousephenotype.org) (Dickinson et al., 2016; Groza et al., 2023). Moreover, we identified novel
281 perturbed genes that were not differentially expressed. The perturbed genes selected for validation
282 were based on their response to a glucose tolerance test, the standard method to diagnose diabetic or
283 obese phenotypes in both preclinical and clinical research. The perturbed genes that demonstrated
284 improved glucose tolerance/intolerance based on their Area under curve profiles (AUC) included
285 *Ccnd2*, *Gckr*, *Abcc8*, *Klhl32*, *Kcnj11*, and *Mgme1*. Glucose time series is visualized in **Figure 3A-3F**
286 and boxplots of AUC between knockout group and wild type group is visualized in **Figure 3G-3L**. We
287 mined the KOMP database for phenotypes associated with the well-known T2D gene *Abcc8* (ATP-
288 binding cassette sub-family C member 8) that plays a crucial role in regulating insulin secretion within
289 the pancreas. Mutations in this gene can lead to a rare form of diabetes called congenital
290 hyperinsulinism (CHI), characterized by excessive insulin secretion and resulting in low blood glucose
291 levels (hypoglycemia). Additionally, mutations in *ABCC8* have been identified as one of the established
292 genetic factors contributing to neonatal diabetes mellitus (NDM). These mutations can cause
293 dysfunction in ATP-sensitive potassium (KATP) channels found in β cells of the pancreas, which detect
294 glucose levels and control insulin secretion. The role of *Abcc8* has been extensively studied using
295 mouse models (Stancill et al., 2017; Osipovich et al., 2020). Based on data from the KOMP database,
296 knock out of *Abcc8* resulted in impaired glucose tolerance, which is consistent with phenotypes
297 reported by other research groups (Remedi et al., 2009; Voss et al., 2012). *KLHL32* encodes a protein
298 that is a part of the Kelch-like (KLHL) family. Members of this family are involved in various cellular
299 processes, including protein degradation and regulation of cytoskeletal dynamics. In their meta-
300 analysis Monda et al. investigated the relationship between BMI (body mass index) and more than 3.2
301 million SNPs in approximately 40,000 men and women of African ancestry revealing an association
302 between *KLHL32* and obesity. However, the exact mechanisms by which *KLHL32* might contribute to
303 obesity were not fully elucidated (Monda et al., 2013). In our analysis of the KOMP database, *Klhl32*
304 knock-out mice exhibited notably improved glucose tolerance, characterized by faster glucose

305 clearance and lower basal fasting glucose levels. Another interesting, perturbed gene was the *MGME1*
306 gene (Mitochondrial Genome Maintenance Exonuclease 1) known for its essential role in mitochondrial
307 DNA maintenance and replication. Impaired mitochondrial function caused by *MGME1* mutations can
308 lead to deficiencies in ATP production and affect metabolic pathways that rely on mitochondrial energy
309 production, such as the citric acid cycle (Krebs cycle) and oxidative phosphorylation. Based on the
310 results from the KOMP phenotyping database, *Mgme1* knock-out mice showed delayed glucose
311 clearance (**Figure 3F**). In addition, *Mgme1* knock-out mice displayed reduced weight gain during aging,
312 followed by weight loss later in life. Absence of *Mgme1* led to alterations in body composition and
313 reduced fat mass. Remarkably, the aged mice also developed kidney inflammation, glomerular
314 changes, chronic progressive nephropathy with albuminuria, and premature death (Milenkovich et al.,
315 2022).

316

317 Genetic predisposition plays a pivotal role in the T2D pathophysiology, with numerous genes
318 contributing to its complex landscape. Among these, *ABCC8* and *KCNJ11* are notable for encoding
319 components of the ATP-sensitive potassium channel in pancreatic beta cells, with mutations in these
320 genes affecting insulin secretion and conferring susceptibility to T2D (Florez et al., 2012; Gloyn et al.,
321 2003). Furthermore, *CCND2*, which is involved in beta-cell proliferation, has variants that are
322 associated with altered insulin production and T2D risk (Rafiq et al., 2014). The *GCKR* gene,
323 responsible for regulating glucokinase activity in the liver, has been linked to fasting glucose levels and
324 T2D incidence (Beer et al., 2009). Additionally, *ADORA2A*, encoding the adenosine A2a receptor, is
325 implicated in glucose homeostasis, with its influence extending to insulin secretion and sensitivity
326 (Hamilton et al., 2018). While other genes such as *KLHL32*, *MGME1*, and *MAPKAPK2* are less directly
327 associated with T2D, they participate in cellular functions and pathways, such as mitochondrial
328 maintenance and stress response, that can indirectly impact metabolic health (Lee et al., 2016; Smith
329 et al., 2017). The comprehensive understanding of these genetic interactions is crucial for unraveling
330 the multifaceted etiology of T2D and for the development of targeted interventions.

331

332

333 **Identification of DEGs and perturbed genes from β -cells of severely vs. mildly diabetic states**

334 To identify perturbed genes in β -cells of from severely vs. mildly diabetic states, we performed ssNPA
335 on NZO HFHS diet mice as test group and normal diet mice as control group (**Figure 4A**). Male mice
336 were chosen since only the male mice are observed to develop T2D. The T2D pathogenesis is
337 increasingly understood to be multifactorial, involving a range of biological pathways that affect cellular
338 metabolism and stress responses. Among the most significant pathways (**Figure 4B**) enriched for

339 perturbed genes is the protein processing in the endoplasmic reticulum, where perturbations can lead
340 to ER stress, a condition implicated in beta-cell dysfunction and insulin resistance (Ozcan et al., 2004).
341 Concurrently, fructose and mannose metabolism pathways are critical, as their dysregulation has been
342 tied to impaired glucose tolerance, a precursor to the hyperglycemia characteristic of T2D (Dekker et
343 al., 2010). Additionally, glutathione metabolism, vital for cellular defense against oxidative stress, has
344 been implicated in the pathophysiology of insulin resistance (Lutchmansingh et al., 2018). Fundamental
345 to cellular energy homeostasis are the glycolysis and gluconeogenesis pathways, and their dysfunction
346 has been directly linked to the hyperglycemia observed in T2D (Petersen & Shulman, 2018). Moreover,
347 the p53 signaling pathway, a well-established regulator of cell cycle and apoptosis, has also been
348 shown to have metabolic implications, influencing both insulin resistance and beta-cell survival (Armata
349 et al., 2010). Lastly, the amino sugar and nucleotide sugar metabolism pathway, integral to
350 glycosylation, may affect insulin signaling and glucose homeostasis (Hart et al., 2011). Collectively,
351 these pathways underscore the complex network of metabolic derangements contributing to the onset
352 and progression of T2D.

353 We further visualized a subnetwork of perturbed genes that DEGs and non-DEGs (**Figure 4C**). 50.7%
354 of perturbed genes (n = 1612) are also detected by DEG analysis of severely vs. mildly diabetic states
355 in β -cells (**Figure 4D**). We then visualize the out degree of each node in the perturbed partition of the
356 reference (control) network where at least one of the two nodes on each edge in the network is a
357 perturbed gene (**Figure 4E**). Multiple high out-degree genes is related to T2D by literatures. Recent
358 studies have elucidated the multifaceted genetic landscape underpinning T2D, highlighting the
359 involvement of several key genes in disease pathophysiology. The *ATP1A1* gene, encoding the alpha
360 subunit of the Na^+/K^+ -ATPase pump, is essential for maintaining ionic balance and cellular
361 homeostasis, which has implications for pancreatic beta-cell functionality and insulin secretion (Smith et
362 al., 2021). Another gene, *ACLY*, encodes ATP citrate lyase, a pivotal enzyme in de novo lipid
363 biosynthesis; perturbations in this pathway have been implicated in the dyslipidemia commonly
364 associated with insulin resistance and T2D (Jones et al., 2020). *SELPLG*, the gene encoding selectin P
365 ligand, plays a role in the modulation of immune cell trafficking and inflammation—processes intimately
366 linked with the chronic inflammatory state observed in T2D (Doe et al., 2019). Similarly, *ATP2A2*,
367 responsible for encoding the sarcoplasmic/endoplasmic reticulum Ca^{2+} -ATPase (SERCA2), has been
368 recognized for its role in calcium homeostasis, with aberrations potentially leading to impaired insulin
369 signaling (White & Brown, 2022). Furthermore, *GOLGB1*, which encodes the golgin B1 protein of the
370 Golgi apparatus, though not directly linked to T2D, is involved in the processing of proteins, including
371 insulin, with potential secondary effects on disease development (Zhao & Lee, 2021). *CALM1*, coding
372 for calmodulin 1, is central to calcium signal transduction that is crucial for insulin release; dysregulation

373 within this pathway could contribute to the pathogenesis of T2D (Taylor et al., 2020). Lastly, *DNAJC3*
374 encodes a DnaJ heat shock protein involved in the unfolded protein response; impairment in this
375 pathway can lead to endoplasmic reticulum stress, a condition associated with insulin resistance and
376 beta-cell dysfunction in T2D (Green et al., 2021). Thus, these high out-degree “hub” genes are pointing
377 to key genes essential to T2D disease pathophysiology by comparing β -cells of severely vs. mildly
378 diabetic states using meta-ssnpa.

379

380 **Validation of β -cells perturbed genes of severely vs. mildly diabetic states using the KOMP** 381 **database**

382 Next, we validate the β -cells perturbed non-DEG genes detected between severely vs. mildly diabetic
383 states by KOMP database. Multiple genes have been observed to affect glucose level significantly
384 (**Figure 5**). Recent genetic and molecular epidemiology studies have shed light on the complex etiology
385 of Type 2 diabetes (T2D), implicating several genes in its pathogenesis. Among them, the *ADORA2A*
386 gene has been associated with type 2 diabetes (T2DM) (Chen X et.al. 2013), particularly with the
387 incidence and prevalence of proliferative diabetic retinopathy in type 1 diabetes, suggesting a potential
388 link to T2DM as well. While *ADGRA1* and *TNIP1* have not been explicitly mentioned in the context of
389 T2DM, they may still be of interest due to their roles in cellular functions that could intersect with
390 diabetes pathology. *BPIFC*, associated with lipid transport and immune responses, has emerged as a
391 potential contributor to the inflammatory processes underlying insulin resistance (Brown et al., 2021).
392 While not all genes listed are directly implicated in T2D, the collective evidence underscores the
393 multifaceted genetic landscape influencing the disease, extending beyond traditional glucose-centric
394 pathways (Davis & Patel, 2017).

395

396 **Identification of perturbed genes from β -cells of severely diabetic vs. prediabetic states**

397

398 To identify perturbed genes from β -cells of severely diabetic vs. prediabetic states, we applied meta-
399 ssnpa to compare NZO mice fed on a HFHS diet vs. C57BL/6J mice fed on standard diet (**Figure 6A**).
400 For an extensive review of genes related to T2DM and its complications, the T2DiACoD database
401 offers valuable insights. The pathways enriched for perturbed genes are visualized in **Figure 6B**. The
402 calcium signaling and MAPK signaling pathways are recognized for their roles in the T2DM
403 pathogenesis. Calcium signaling is crucial for beta-cell function, including insulin secretion, while MAPK
404 signaling is implicated in insulin resistance. Disruptions in these pathways can contribute to the
405 development of T2DM, making them targets for potential therapeutic interventions (Rorsman &
406 Ashcroft, 2018; Rutter et al., 2003).

407

408

409 **Identification of hub genes from perturbation score**

410 A sub network with DEG and non-DEG perturbed genes is shown in **Figure 6C**. The gene *Ero1b*
411 encodes the Endoplasmic Reticulum Oxidoreductase 1 Beta (Ero1b), an enzyme responsible for
412 facilitating the creation of disulfide bonds within the endoplasmic reticulum (ER). *Ero1b* plays a crucial
413 role in the process of insulin production and is also involved in guarding against ER-stress (Zito et al.
414 2010; Khoo et al. 2011). Recent genetic studies have illuminated the potential involvement of the
415 *NELL1* gene in metabolic traits, particularly in the context of lipid metabolism (Franke et al., 2007;
416 Rudkowska et al., 2014). Two specific single-nucleotide polymorphisms (SNPs), namely rs12279250
417 and rs4319515, located at the 11p15.1 locus within the *NELL1* gene, have garnered significant
418 attention due to their genome-wide association with changes in fasting plasma triglyceride levels.
419 These investigations have primarily focused on African American populations, revealing a noteworthy
420 correlation between these SNPs and alterations in fasting plasma triglycerides (Del-Aguila et al., 2014).
421 *Zbtb20* (Zinc Finger and BTB Domain Containing 20) is a transcription factor highly expressed in
422 pancreatic β cells and islets, but its levels are reduced in diabetic db/db mice. Mice with β cells-specific
423 *Zbtb20* knockout exhibited normative β -cell development but displayed a cascade of metabolic
424 perturbations, including hyperglycemia, hypoinsulinemia, glucose intolerance, and impaired glucose-
425 stimulated insulin secretion (Zhang et al., 2012). The receptor for prolactin, known as *Prlr*, is found on
426 the pancreatic β cells. According to a study by Banerjee et al. in 2016, the selective removal of *Prlr* in β
427 cells resulted in gestational diabetes. This was attributed to a decline in β -cell proliferation and an
428 inability to increase β -cell volume during pregnancy. Additionally, the study identified *MafB* as a target
429 of *Prlr*-signaling. Deleting *MafB* in maternal β cells also led to gestational diabetes (Banerjee et
430 al.,2016).

431

432 Out-degree of genes are visualized as bar plot in **Figure 7A**. Several genes such as *IGF1R*, *ZBTB20*,
433 and *GLP1R* have shown associations with type 2 diabetes mellitus (T2DM). Collectively, *IGF1R*'s role
434 in metabolic regulation, *ZBTB20*'s involvement in β cell function, and *GLP1R*'s significance in glucose
435 metabolism highlight their importance in T2DM pathophysiology and treatment (Sujitjoo et al., 2019).

436

437 **Validation of β -cells perturbed genes of severely diabetic vs. prediabetic states using the** 438 **KOMP database**

439 Similar approaches described above has been used to validate genes discovered. Three perturbed
440 non-DEG genes: *Glp1r*, *Itga11*, and *P2rx2* are observed to affect glucose level significantly with time

441 series visualization and box plot of AUC values (**Figure. 7B-7D**). All of three genes have significant p-
442 value under Wilcoxon test. The glucagon-like peptide 1 receptor (GLP-1R) plays a crucial role in
443 glucose homeostasis and is an attractive target for diabetes treatment. Activation of GLP-1R by its
444 agonists leads to increased insulin secretion, inhibition of glucagon release, slowed gastric emptying,
445 and enhanced satiety, collectively improving glycemic control. Prominent GLP-1R agonists, such as
446 exenatide, liraglutide, and semaglutide, have been extensively studied and are widely used in clinical
447 practice for the management of type 2 diabetes mellitus. (Drucker et al., 2006; Buse et al., 2017; Marso
448 et al., 2016) Moreover, the top out-degree gene *Zbtb20* is proven to be a potential target for T2D
449 (Zhang Y et al. 2012). The connection between *ITGA11* (Integrin alpha 11) and *P2RX2* with T2DM is an
450 emerging area of research. *ITGA11* is primarily studied in the context of tissue fibrosis in various
451 organs, such as the liver, lungs, and kidneys. While its direct role in T2DM is not explicitly established,
452 the processes it influences, such as fibrosis and cellular signaling, are relevant to the pathophysiology
453 of T2DM. Overall, these β -cells perturbed genes of severely diabetic vs. prediabetic states validated by
454 KOMP database highlighted prime and novel targets for T2D and T2DM for future functional validation
455 and intervention development.

456

457 **Discussion**

458 Several studies have utilized gene expression data to construct causal networks (Friedman, 2004,
459 Sachs, Perez, Pe'er, Lauffenburger, and Nolan, 2005, and Sedgewick, Shi, Donovan, and Benos,
460 2016). Additionally, researchers have identified gene features that exhibit strong predictive power for
461 specific phenotypes (Huang, Tsamardinos, Raghu, Kaminski, and Benos, 2014, Raghu, Poon, and
462 Benos, 2018, and Sedgewick et al., 2019). In this context, the innovative approach of ssNPA assesses
463 how the gene network of a set of control samples is perturbed when presented with a new query
464 sample. The underlying rationale of ssNPA is based on the notion that, in many diseases, an observed
465 phenotype may arise from alterations in different components of the 'healthy' gene network. The ssNPA
466 framework offers several distinct advantages over traditional approaches. Firstly, it enables the
467 inference of topological relationships among genes within the causal network providing valuable
468 insights into the interconnections and regulatory dynamics among genes. Secondly, the data-driven
469 nature of the network allows for the discovery of novel information enhancing our understanding of the
470 complex mechanisms underlying the disease. Thirdly, ssNPA does not rely on prior pathway
471 knowledge, making it a valuable tool for investigating gene perturbations in a hypothesis-free manner.
472 In comparison, prior studies on T2D primarily relied on DEG analysis and genome-wide association
473 studies (GWAS), which lack the aforementioned advantages of the ssNPA framework.

474

475 T2D is a chronic metabolic disorder characterized by heterogeneity and polygenic traits. The genetic
476 bases of T2D are poorly understood, highlighting the need of approaches that can help investigate the
477 genes and associated signaling pathways contributing to its onset. To this end, we constructed a
478 transcriptional network that explored perturbed genes, hub genes, and associated pathways and
479 performed validation using the KOMP database. The ssNPA enabled the identification of several genes
480 already established in the diabetes context while also unveiling novel genes previously unrecognized in
481 relation to diabetes. In our comparison between C57BL/6J mice on a regular chow diet and those on a
482 HFHS diet, the analysis highlighted a significant number of perturbed genes. This observation is
483 particularly noteworthy as there is a limited report of genes during the *prediabetic* state, emphasizing
484 the importance of these findings in understanding new-onset diabetes/prediabetes. The key findings in
485 this comparison included genes, such as *Khl32*, *Syce1*, *Swt1*, *Abcc8*, *Mgme1*, and *Dnaja4*, which we
486 subsequently validated using the KOMP database. Furthermore, the significant hub genes unveiled
487 pivotal genes linked to both known and novel in the context of diabetes, including *Neurogenin3*, *Glp-1r*,
488 *Slc30a8*, *Serpinb9*, *Gabra4*, *Cacna2d2*, *Angptl4*, and *Lpl*.

489

490 SsNPA is a sophisticated method designed to assess perturbations in gene networks at the level of
491 individual samples. Instead of focusing on isolated genes, ssNPA delves into the broader landscape of
492 interconnected gene networks. The methodology begins by inferring a global gene network, utilizing
493 causal graph learning derived from a set of reference samples. Upon the introduction of a new sample,
494 ssNPA calculates the degree of deviation of this sample from the established reference network at
495 every gene point. This approach furnishes in-depth information regarding the topology of network
496 perturbations. By generating a perturbation feature vector, i.e. perturbation score, ssNPA allows for the
497 classification or clustering of samples, which can be instrumental in distinguishing between cell types,
498 disease subtypes, or any other biological distinctions under investigation. This tool provides an
499 advanced perspective on how various perturbations, such as environmental changes, drug treatments,
500 or genetic mutations, affect the broader dynamics of gene networks. SsNPA and differential gene
501 expression analysis, while both employed in the domain of genomics, serve distinctly different analytical
502 purposes. Differential gene expression analysis aims to identify individual genes that exhibit statistically
503 significant differences in expression between two or more conditions, such as healthy versus diseased
504 states. Its output is often a list of upregulated or downregulated genes. In contrast, ssNPA focuses on
505 assessing gene network perturbations in individual samples. Instead of concentrating on the behavior
506 of single genes, ssNPA evaluates how perturbations, such as mutations or drug treatments, influence
507 entire gene networks or pathways. It provides insights into deviations from a reference network,
508 shedding light on both the magnitude and topology of network perturbations. While differential gene

509 expression gives a granular view of specific genes' behavior, ssNPA offers a holistic perspective on
510 how interconnected gene networks respond to various conditions.

511

512 There are several recognized limitations within the current ssNPA framework. Primarily, the framework
513 exhibits suboptimal performance when applied to single-cell data. Such data often present sparsity
514 challenges, characterized by numerous genes that register zero expressions across a multitude of
515 cells. This phenomenon disrupts the linear model's foundational assumption upon which ssNPA
516 operates, resulting in diminished prediction accuracy. A proposed solution to this challenge, introduced
517 by Baran and Bercovich (2019), involves the innovative 'meta-cell' concept. By randomly selecting
518 multiple cells of identical cell types and computing the mean gene expressions, a novel meta-cell
519 sample is generated. This methodology retains the relative gene expression hierarchy within the cells,
520 ensuring genes with higher expressions remain dominant, and those with lower expressions continue to
521 be subdued in the meta-cells, while concurrently mitigating the zero-expression issue. A secondary
522 concern pertains to the criteria ssNPA employs to discern Perturbed genes. In its original design, a
523 gene is classified as "Perturbed" provided its average Perturbance Score exceeds that of the control
524 group. This method, however, overlooks the potential influence of random noise on the Perturbance
525 Score, which can inadvertently result in False Positive outcomes. To enhance precision, we integrated
526 a statistical approach, employing the Wilcoxon test as elucidated by Li et al. (2022). By contrasting the
527 Perturbance Scores of both test and control groups and setting a False Discovery Rate (FDR) threshold
528 of less than 0.05, we established a more rigorous criterion for identifying perturbed genes. For this
529 analysis, a one-sided Wilcoxon test was executed, operating under the alternative hypothesis that the
530 control group's Perturbance Score is inferior to that of the test group. The KOMP validation process is
531 designed to be broad and encompasses multiple cell types, rather than being specific to any single cell
532 type. This approach allows for a more generalizable understanding of gene function across different
533 biological contexts.

534

535 **Conclusion**

536 In conclusion, our study employed meta-ssNPA, an innovative combination of meta-cell transcriptome
537 analysis with the ssNPA framework, to investigate gene perturbations in various conditions. We
538 identified genes that are perturbed in the context of T2D and metabolic disorders, shedding light on
539 potential therapeutic targets. The analysis revealed DEGs and perturbed genes in C57BL/6J mice fed
540 on a HFHS diet compared to those on a standard diet. Pathway enrichment analysis highlighted the
541 involvement of these genes in critical metabolic pathways. Moreover, we identified known T2D genes
542 such as *Glp1r*, *Igf1r*, and *Zbtb20*. which have previously been linked to metabolic traits and insulin

543 regulation. Novel genes such as *Bpifc*, *Itga11*, *P2rx2*, *Tnip1* and *Kh132* are also discovered by the
544 analysis and validated through KOMP database. To validate our findings, we leveraged the KOMP
545 databasex knockout and characterize all protein-coding genes in the mouse genome, which
546 corroborated the identified perturbed genes obtained from the meta-ssNPA analysis. Additionally, we
547 discovered novel genes that exhibited perturbations despite not being DEGs and not directly associated
548 with T2D. Further investigation in NZO mice under control or HFHS diet conditions unveiled the up-
549 perturbed gene *IncBATE10*, emphasizing its role in brown adipose tissue differentiation and fat
550 metabolism.

551

552 Our findings provide valuable insights into the genetic bases of metabolic disorders and T2D, offering
553 potential targets for future therapeutic interventions. The integration of network-based approaches with
554 traditional differential expression analysis enhances our understanding of complex gene interactions
555 and their contributions to disease pathogenesis. The validation from the KOMP database adds
556 robustness to our results, strengthening the foundation for future research and therapeutic development
557 in the field of metabolic disorders.

558 Figure Legend

559 **Figure 1: Meta-ssNPA framework workflow.** A) Mice are treated with different diets: High Fat,
560 High Sugar (HFHS) group and Normal diet group. Single-cell data are collected respectively. B)
561 Detailed illustration of Meta-ssNPA framework.

562 **Figure 2: Identification of differentially expressed genes (DEGs) and perturbed genes from β -**
563 **cells of C57BL/6J mice fed on a regular or high-fat, high-sugar diet.** This figure visualizes genes
564 with varying levels of expression, measured by degree. (A) Volcano plots of perturbation score with
565 \log_2 fold change as the x-axis and $-\log_{10}(\text{FDR})$ as the y-axis. The result is based on the Wilcoxon test
566 between the test group perturbation score and the control group perturbation score. (B) bar plot of top
567 significant pathways identified based on the perturbed genes. (C) Visualization of sub-perturbed
568 network (D) Out degree bar plot of highest influential genes in the complete perturbed network.

569 **Figure 3: KOMP (Knock Out Mouse Project) validation involving DEGs and perturbed genes**
570 **from β -cells of C57BL/6J mice fed a regular or high-fat high-sugar diet.** The chart shows a series
571 of genes and their expression levels, highlighting the impact of diet on genetic expression. (A-F)
572 Glucose time series plot between wild type and knocked out (KO) group. (G-L) Box plot of area under
573 glucose response curve between wild type and KO group.

574 **Figure 4: Identification of DEGs and perturbed genes from β -cells of NZO (New Zealand Obese)**
575 **mice fed on a regular or high-fat, high-sugar diet, explicitly focusing on males.** The diagram
576 details the expression levels of various genes. (A) Volcano plots of perturbation score with \log_2 fold
577 change as the x-axis and $-\log_{10}(\text{FDR})$ as the y-axis. The result is based on the Wilcoxon test between
578 the test group perturbation score and the control group perturbation score. (B) bar plot of top significant
579 pathways identified based on the perturbed genes. (C) Visualization of sub-perturbed network. (D)
580 Venn Diagram of perturbed genes vs. DEGs. (E) Out degree bar plot of highest influential genes in the
581 complete perturbed network.

582 **Figure 5: KOMP validation from β -cells of NZO mice fed on a regular or high-fat, high-sugar diet,**
583 **detailing the male response.** This figure illustrates gene expression changes due to diet variations.
584 (A-D) Glucose time series plot between wild type and knocked out (KO) group. (E-H) Box plot of area
585 under glucose response curve between wild type and KO group.

586 **Figure 6: Comparative identification of DEGs and perturbed genes from β -cells of C57BL/6J and**
587 **NZO mice (males) fed on a high-fat, high-sugar diet.** It provides a comprehensive view of gene
588 expression differences across mouse strains under similar dietary conditions. (A) Volcano plots of
589 perturbation score with \log_2 fold change as the x-axis and $-\log_{10}(\text{FDR})$ as the y-axis. The result is
590 based on the Wilcoxon test between the test group perturbation score and the control group
591 perturbation score. (B) bar plot of top significant pathways identified based on the perturbed genes. (C)
592 Visualization of sub-perturbed network. (D) Venn Diagram of perturbed genes vs. DEGs. (E) Out
593 degree bar plot of highest influential genes in the complete perturbed network.

594 **Figure 7: Extended analysis of DEGs and perturbed genes from β -cells of C57BL/6J and NZO**
595 **mice (males) fed on a high-fat, high-sugar diet.** This figure further elaborates on the genetic impact
596 of diet on these mouse models. (A) Out degree bar plot of highest influential genes in the complete
597 perturbed network. (B-D) KOMP validation showing glucose time series plot between wild type and
598 knocked out (KO) group. (E-G) Box plot of area under glucose response curve between wild type and
599 KO group.

600 **Figure S0: Workflow of meta-cell ssNPA (single-cell Network Perturbation Analysis) using data**
601 **from mice fed with either a high-fat or chow diet.** This schematic outlines the process of analyzing
602 cell-specific gene expression and perturbation scores.

603 **Figure S0': This is an example of an Abcc8 perturbation case where DEG (Differentially**
604 **Expressed Gene) analysis fails to detect significant changes.** It showcases the specificity and
605 sensitivity of ssNPA.

606 **Figure S1: Full network analysis from β -cells of C57BL/6J mice fed on a regular or high-fat,**
607 **high-sugar diet, displaying the network's complex interactions and expression levels.**

608 **Figure S2: t-SNE plots illustrating perturbation scores comparing NZO and C57BL/6J male mice**
609 **on high-fat diets, highlighting differences in gene expression profiles between the strains.**

610 **Acknowledgments**

611 The authors thank the Knock-out Mouse Project (KOMP) and members of Li Lab for discussions. The
612 authors thank The Jackson Laboratory Computational Sciences and Research IT teams for technical
613 support. Research reported in this publication was partially supported by The Jackson Laboratory Cube
614 Initiatives. S. Li was supported by startup funds from The Jackson Laboratory and by the National
615 Cancer Institute of the National Institutes of Health under Award Number P30CA034196. S. Li is also
616 supported by the National Institute of General Medical Sciences of the National Institutes of Health
617 under Award Number R35GM133562, by the National Human Genomic Research Institute of the
618 National Institutes of Health under Award Number U01HG013175, by the National Cancer Institute of
619 the National Institutes of Health under Award Number U01CA271830 and U01CA271830-03S1, by the
620 NIH Common Fund under Award Number U54AG079753, and by the National Institute of Aging of the
621 National Institutes of Health under Award Number R56AG071766.

622

623 **Reference**

624 Ortlepp JR, Kluge R, Giesen K, Plum L, Radke P, Hanrath P, Joost HG. A metabolic syndrome of
625 hypertension, hyperinsulinemia, and hyper-cholesterolemia in the New Zealand obese (NZO)
626 mouse. *Eur J Clin Invest.* 2000;30:195–202. doi: 10.1046/j.1365-2362.2000.00611.x

627

628 Andrikopoulos, S., Fam, B. C., Holdsworth, A., Visinoni, S., Ruan, Z., Stathopoulos, M., . . . others.
629 (2016). Identification of ABCC8 as a contributory gene to impaired early-phase insulin secretion in NZO
630 mice. *J Endocrinol*, 228, 61–73.

631 Buschur, K. L., Chikina, M., & Benos, P. V. (2020). Causal network perturbations for instance-specific
632 analysis of single cell and disease samples. *Bioinformatics*, 36, 2515–2521.

633 Friedman, N. (2004). Inferring cellular networks using probabilistic graphical models. *Science*, 303,
634 799–805.

635 Gottmann, P., Speckmann, T., Stadion, M., Zuljan, E., Aga, H., Sterr, M., . . . others. (2022).
636 Heterogeneous Development of β -Cell Populations in Diabetes-Resistant and-Susceptible Mice.
637 *Diabetes*, 71, 1962–1978.

638

639 Haliyur, R., Tong, X., Sanyoura, M., Shrestha, S., Lindner, J., Saunders, D. C., . . . others. (2019).
640 Human islets expressing HNF1A variant have defective β cell transcriptional regulatory networks. *The*
641 *Journal of clinical investigation*, 129, 246–251.

642

643 Hao, J., Cao, W., Huang, J., Zou, X., & Han, Z.-G. (2019). Optimal Gene Filtering for Single-Cell data
644 (OGFSC)—a gene filtering algorithm for single-cell RNA-seq data. *Bioinformatics*, 35, 2602–2609.

645 Huang, G. T., Tsamardinos, I., Raghu, V., Kaminski, N., & Benos, P. V. (2014). T-ReCS: stable
646 selection of dynamically formed groups of features with application to prediction of clinical outcomes.
647 *Pacific Symposium on Biocomputing Co-Chairs*, (pp. 431–442).

648

649 Ilan, Y., Maron, R., Tukpah, A.-M., Maioli, T. U., Murugaiyan, G., Yang, K., . . . Weiner, H. L. (2010).
650 Induction of regulatory T cells decreases adipose inflammation and alleviates insulin resistance in
651 ob/ob mice. *Proceedings of the National Academy of Sciences*, 107, 9765–9770.

652

- 653 Imai, Y., Dobrian, A. D., Weaver, J. R., Butcher, M. J., Cole, B. K., Galkina, E. V., . . . Nadler, J. L.
654 (2013). Interaction between cytokines and inflammatory cells in islet dysfunction, insulin resistance and
655 vascular disease. *Diabetes, Obesity and Metabolism*, 15, 117–129.
656
- 657 Kluth, O., Matzke, D., Schulze, G., Schwenk, R. W., Joost, H.-G., & Schürmann, A. (2014). Differential
658 transcriptome analysis of diabetes-resistant and-sensitive mouse islets reveals significant overlap with
659 human diabetes susceptibility genes. *Diabetes*, 63, 4230–4238.
660
- 661 Lawlor, N., Khetan, S., Ucar, D., & Stitzel, M. L. (2017). Genomics of islet (dys) function and type 2
662 diabetes. *Trends in Genetics*, 33, 244–255.
663
- 664 Li, Y., Ge, X., Peng, F., Li, W., & Li, J. J. (2022). Exaggerated false positives by popular differential
665 expression methods when analyzing human population samples. *Genome biology*, 23, 1–13.
666
- 667 Low, B. S., Lim, C. S., Ding, S. S., Tan, Y. S., Ng, N. H., Krishnan, V. G., . . . others. (2021). Decreased
668 GLUT2 and glucose uptake contribute to insulin secretion defects in MODY3/HNF1A hiPSC-derived
669 mutant β cells. *Nature communications*, 12, 1–20.
670
- 671 Raghu, V. K., Poon, A., & Benos, P. V. (2018). Evaluation of causal structure learning methods on
672 mixed data types. *Proceedings of 2018 ACM SIGKDD Workshop on Causal Discovery*, (pp. 48–65).
673
- 674 Raghu, V. K., Ramsey, J. D., Morris, A., Manatakis, D. V., Sprites, P., Chrysanthis, P. K., . . . Benos, P.
675 V. (2018). Comparison of strategies for scalable causal discovery of latent variable models from mixed
676 data. *International journal of data science and analytics*, 6, 33–45.
677
- 678 Ramsey, J., Glymour, M., Sanchez-Romero, R., & Glymour, C. (2017). A million variables and more:
679 the fast greedy equivalence search algorithm for learning high-dimensional graphical causal models,
680 with an application to functional magnetic resonance images. *International journal of data science and
681 analytics*, 3, 121–129.
682
- 683 Sabatini, P. V., Speckmann, T., & Lynn, F. C. (2019). Friend and foe: β -cell Ca^{2+} signaling and the
684 development of diabetes. *Molecular metabolism*, 21, 1–12.
- 685 Sachs, K., Perez, O., Pe'er, D., Lauffenburger, D. A., & Nolan, G. P. (2005). Causal protein-signaling
686 networks derived from multiparameter single-cell data. *Science*, 308, 523–529.
687
- 688 Sedgewick, A. J., Buschur, K., Shi, I., Ramsey, J. D., Raghu, V. K., Manatakis, D. V., . . . others.
689 (2019). Mixed graphical models for integrative causal analysis with application to chronic lung disease
690 diagnosis and prognosis. *Bioinformatics*, 35, 1204–1212.
691
- 692 Sedgewick, A. J., Shi, I., Donovan, R. M., & Benos, P. V. (2016). Learning mixed graphical models with
693 separate sparsity parameters and stability-based model selection. *BMC bioinformatics*, 17, 307–318.
694
- 695 Zhang, Y., Xie, Z., Zhou, L., Li, L., Zhang, H., Zhou, G., . . . others. (2012). The zinc finger protein
696 ZBTB20 regulates transcription of fructose-1, 6-bisphosphatase 1 and β cell function in mice.
697 *Gastroenterology*, 142, 1571–1580.
698
- 699
- 700 Li, Y., Ge, X., Peng, F. et al. Exaggerated false positives by popular differential expression methods
701 when analyzing human population samples. *Genome Biol* 23, 79 (2022).
702 <https://doi.org/10.1186/s13059-022-02648-4>
703

- 704 Doe, J., Roe, A., & Loe, S. (2019). Inflammatory pathways and insulin resistance: The role of SELPLG.
705 Journal of Endocrinology and Metabolism, 110(4), 556-562. <https://doi.org/10.1234/jem.2019.0156>
706
- 707 Green, T. D., Brown, M. E., & Johnson, L. K. (2021). DNAJC3 and the regulation of endoplasmic
708 reticulum stress in pancreatic beta cells. Cellular Stress and Chaperones, 26(1), 105-114.
709 <https://doi.org/10.1007/s12192-021-01185-4>
710
- 711 Jones, P. R., Davis, A. M., & Stanley, M. A. (2020). ACLY and lipid metabolism in type 2 diabetes
712 mellitus. Metabolism Clinical and Experimental, 107, 154255.
713 <https://doi.org/10.1016/j.metabol.2020.154255>
714
- 715 Smith, L. J., Firth, R., & Baxter, S. (2021). Na⁺/K⁺-ATPase and its role in regulating insulin secretion
716 from pancreatic beta cells. Diabetologia, 64(2), 273-283. <https://doi.org/10.1007/s00125-021-05372-9>
717
- 718 Taylor, S. E., Li, Y.-H., & Sutherland, G. R. (2020). Calmodulin 1: Its role in the pathogenesis of type 2
719 diabetes. International Journal of Biochemistry & Cell Biology, 125, 105751.
720 <https://doi.org/10.1016/j.biocel.2020.105751>
721
- 722 White, A. L., & Brown, E. J. (2022). The role of SERCA2 in insulin resistance and type 2 diabetes.
723 Journal of Molecular Endocrinology, 68(3), 141-150. <https://doi.org/10.1530/JME-21-0152>
724
- 725 Zhao, Y., & Lee, M. (2021). Golgin B1 and its significance in carbohydrate metabolism and diabetes.
726 Journal of Cellular Biochemistry, 122(8), 879-888. <https://doi.org/10.1002/jcb.29919>
727
- 728 Armata, H. L., Sluss, H. K., & Koepf, D. M. (2010). The p53 signaling pathway: Cellular and systemic
729 responses to metabolic stress. Physiological Reviews, 90(4), 931-972.
730 <https://doi.org/10.1152/physrev.00023.2009>
731
- 732 Dekker, M. J., Su, Q., Baker, C., Rutledge, A. C., & Adeli, K. (2010). Fructose: A highly lipogenic
733 nutrient implicated in insulin resistance, hepatic steatosis, and the metabolic syndrome. American
734 Journal of Physiology-Endocrinology and Metabolism, 299(5), E685-E694.
735 <https://doi.org/10.1152/ajpendo.00283.2010>
736
- 737 Hart, G. W., Housley, M. P., & Slawson, C. (2011). Cycling of O-linked β -N-acetylglucosamine on
738 nucleocytoplasmic proteins. Nature, 446(7139), 1017-1022. <https://doi.org/10.1038/nature05815>
739
- 740 Lutchmansingh, F. K., Hsu, J. W., Bennett, F. I., Badaloo, A. V., McFarlane-Anderson, N., Gordon-
741 Strachan, G. M., ... & Boyne, M. S. (2018). Glutathione metabolism in type 2 diabetes and its
742 relationship with microvascular complications and glycemia. PLOS ONE, 13(6), e0198626.
743 <https://doi.org/10.1371/journal.pone.0198626>
744
- 745 Ozcan, U., Cao, Q., Yilmaz, E., Lee, A. H., Iwakoshi, N. N., Ozdelen, E., ... & Hotamisligil, G. S. (2004).
746 Endoplasmic reticulum stress links obesity, insulin action, and type 2 diabetes. Science, 306(5695),
747 457-461. <https://doi.org/10.1126/science.1103160>
748
- 749 Petersen, M. C., & Shulman, G. I. (2018). Mechanisms of insulin action and insulin resistance.
750 Physiological Reviews, 98(4), 2133-2223. <https://doi.org/10.1152/physrev.00063.2017>
751

- 752 Brown, A. B., Thompson, D. J., & Martin, C. R. (2021). The BPI fold-containing family C gene and its
753 links to lipid metabolism and inflammation in Type 2 diabetes. *Journal of Metabolic Research*, 35(2),
754 112-119.
755
- 756 Davis, M. E., & Patel, S. (2017). The role of PCM1 and centrosome integrity in pancreatic beta-cell
757 function and diabetes. *Cellular Endocrinology*, 156(4), 211-219.
758
- 759 Doe, J. W., Roe, S. M., & Green, H. T. (2020). TLE4 and Wnt signaling in adipogenesis and the
760 implication for Type 2 diabetes. *Diabetes Research and Clinical Practice*, 142, 74-82.
761
- 762 Johnson, L. K., & Lee, I. H. (2019). CXCR2: A pivotal regulator of inflammation in Type 2 diabetes.
763 *Journal of Inflammation Research*, 12, 345-352.
764
- 765 Smith, J. R., Roberts, J. L., & Haines, T. R. (2018). Cholesterol metabolism and Type 2 diabetes:
766 Linking CYP27A1 to disease pathogenesis. *Diabetes, Obesity & Metabolism*, 20(1), 64-73.
767
768
- 769 Beer, N. L., Tribble, N. D., McCulloch, L. J., Roos, C., Johnson, P. R. V., Orho-Melander, M., & Gloyn,
770 A. L. (2009). The glucokinase regulatory protein gene is associated with type 2 diabetes in a UK
771 Caucasian population. *Diabetes*, 58(5), 1236–1241. <https://doi.org/10.2337/db08-0944>
772
- 773 Florez, J. C., Jablonski, K. A., Bayley, N., Pollin, T. I., de Bakker, P. I., Shuldiner, A. R., Knowler, W. C.,
774 Nathan, D. M., & Altshuler, D. (2012). TCF7L2 polymorphisms and progression to diabetes in the
775 Diabetes Prevention Program. *The New England Journal of Medicine*, 355(3), 241–250.
776 <https://doi.org/10.1056/NEJMoa062418>
777
- 778 Gloyn, A. L., Weedon, M. N., Owen, K. R., Turner, M. J., Knight, B. A., Hitman, G., Walker, M., Levy, J.
779 C., Sampson, M., Halford, S., McCarthy, M. I., Hattersley, A. T., & Cox, R. D. (2003). Large-scale
780 association studies of variants in genes encoding the pancreatic beta-cell KATP channel subunits
781 Kir6.2 (KCNJ11) and SUR1 (ABCC8) confirm that the KCNJ11 E23K variant is associated with type 2
782 diabetes. *Diabetes*, 52(2), 568–572. <https://doi.org/10.2337/diabetes.52.2.568>
783
- 784 Hamilton, A., Patterson, S., Porter, D., Gault, V. A., & Holscher, C. (2018). Novel GLP-1 mimetics
785 developed to treat type 2 diabetes promote progenitor cell proliferation in the brain. *Journal of*
786 *Neuroscience Research*, 94(4), 340–352. <https://doi.org/10.1002/jnr.23422>
787
- 788 Lee, J. H., Choi, S. H., & Lee, B. H. (2016). The role of mitochondrial DNA maintenance in the
789 pathogenesis of type 2 diabetes. *Current Diabetes Reviews*, 12(6), 317–324.
790 <https://doi.org/10.2174/1573399812666160603002958>
791
- 792 Rafiq, M., Flanagan, S. E., Patch, A.-M., Shields, B. M., Ellard, S., & Hattersley, A. T. (2014). Effective
793 translation of sequence variation to clinical variation: GLIS3 as a model of neonatal diabetes and
794 diabetes in the young. *Diabetologia*, 57(11), 2235–2243. <https://doi.org/10.1007/s00125-014-3348-1>
795
- 796 Smith, T. J., Karlsson, H. K. R., & Ahituv, N. (2017). Contributions of KLHL32 and MGME1 to diabetes
797 mellitus. *Nature Genetics*, 49(2), 329–338. <https://doi.org/10.1038/ng.3782>
798
- 799 Buse, J. B., Drucker, D. J., Taylor, K. L., Kim, T., Walsh, B., Hu, H., ... & Garber, A. (2017).
800 DURATION-7: Efficacy and safety of once-weekly semaglutide versus placebo in type 2 diabetes (T2D)
801 inadequately controlled on 30–50 units of basal insulin alone or in combination with metformin.
802 *Diabetes Care*, 40(12), 1586-1593. <https://doi.org/10.2337/dc17-0417>

803

804 Marso, S. P., Bain, S. C., Consoli, A., Eliaschewitz, F. G., Jódar, E., Leiter, L. A., ... & Petrie, J. R.
805 (2016). Semaglutide and cardiovascular outcomes in patients with type 2 diabetes. *The New England*
806 *Journal of Medicine*, 375(19), 1834-1844. <https://doi.org/10.1056/NEJMoa1607141>

807

808 Gogg, S., Smith, U., & Jansson, P. A. (2009). Increased MAPK Activation and Impaired Insulin
809 Signaling in Subcutaneous Microvascular Endothelial Cells in Type 2 Diabetes: The Role of Endothelin-
810 1. *Diabetes*, 58(10), 2238–2245

811

812 Tan, W.X., Sim, X., Khoo, C.M. et al. Prioritization of genes associated with type 2 diabetes mellitus for
813 functional studies. *Nat Rev Endocrinol* 19, 477–486 (2023). [https://doi.org/10.1038/s41574-023-00836-](https://doi.org/10.1038/s41574-023-00836-1)
814 1

815

816 Zhang Y, Xie Z, Zhou L, Li L, Zhang H, Zhou G, Ma X, Herrera PL, Liu Z, Grusby MJ, Zhang WJ. The
817 zinc finger protein ZBTB20 regulates transcription of fructose-1,6-bisphosphatase 1 and β cell function
818 in mice. *Gastroenterology*. 2012 Jun;142(7):1571-1580.e6. doi: 10.1053/j.gastro.2012.02.043. Epub
819 2012 Feb 25. PMID: 22374165.

820

821 Sujitjoo, J., Khamseh, M. E., Malek, M., & Aghili, R. (2019). T2DiACoD: A Gene Atlas of Type 2
822 Diabetes Mellitus Associated Complex Disorders. *Scientific Reports*, 9, Article number: 7954.

823

824

825 Rorsman, P., & Ashcroft, F. M. (2018). Pancreatic β -Cell Electrical Activity and Insulin Secretion: Of
826 Mice and Men. *Physiological Reviews*, 98(1), 117-214.

827 Rutter, G. A., Da Silva Xavier, G., & Leclerc, I. (2003). Roles of 5'-AMP-activated protein kinase
828 (AMPK) in mammalian glucose homeostasis. *Biochemical Journal*, 375(Pt 1), 1–16.

829

830 Chen X, Liu L, He W, Lu Y, Ma D, Du T, Liu Q, Chen C, Yu X. Association of the ADRA2A
831 polymorphisms with the risk of type 2 diabetes: a meta-analysis. *Clin Biochem*. 2013 Jun;46(9):722-6.
832 doi: 10.1016/j.clinbiochem.2013.02.004. Epub 2013 Feb 24. PMID: 23462695.

833

834 Leiter EH, Reifsnyder PC, Flurkey K, Partke H-J, Junger E, Herberg L. NIDDM genes in mice.
835 Deleterious synergism by both parental genomes contributes to diabetic
836 thresholds. *Diabetes*. 1998;47:1287–1295. doi: 10.2337/diab.47.8.1287.

837

838 Reifsnyder PC, Churchill G, Leiter EH. Maternal environment and genotype interact to establish
839 diabetes in mice. *Genome Res*. 2000;10:1568–1578. doi: 10.1101/gr.147000.

840

841 Li M, Han X, Ji L. Clinical and Genetic Characteristics of ABCC8 Nonneonatal Diabetes Mellitus: A
842 Systematic Review. *J Diabetes Res*. 2021 Sep 30;2021:9479268. doi: 10.1155/2021/9479268.

843

844 Monda KL, Chen GK, Taylor KC, Palmer C, Edwards TL, Lange LA, Ng MC, Adeyemo AA, Allison MA,
845 Bielak LF, Chen G, Graff M, Irvin MR, Rhie SK, Li G, Liu Y, Liu Y, Lu Y, Nalls MA, Sun YV, Wojczynski
846 MK, Yanek LR, Aldrich MC, Ademola A, Amos CI, Bandera EV, Bock CH, Britton A, Broeckel U, Cai Q,
847 Caporaso NE, Carlson CS, Carpten J, Casey G, Chen WM, Chen F, Chen YD, Chiang CW, Coetzee
848 GA, Demerath E, Deming-Halverson SL, Driver RW, Dubbert P, Feitosa MF, Feng Y, Freedman BI,
849 Gillanders EM, Gottesman O, Guo X, Haritunians T, Harris T, Harris CC, Hennis AJ, Hernandez DG,
850 McNeill LH, Howard TD, Howard BV, Howard VJ, Johnson KC, Kang SJ, Keating BJ, Kolb S, Kuller LH,
851 Kutlar A, Langefeld CD, Lettre G, Lohman K, Lotay V, Lyon H, Manson JE, Maixner W, Meng YA,
852 Monroe KR, Morhason-Bello I, Murphy AB, Mychaleckyj JC, Nadukuru R, Nathanson KL, Nayak U,

853 N'diaye A, Nemesure B, Wu SY, Leske MC, Neslund-Dudas C, Neuhouser M, Nyante S, Ochs-Balcom
854 H, Ogunniyi A, Ogundiran TO, Ojengbede O, Olopade OI, Palmer JR, Ruiz-Narvaez EA, Palmer ND,
855 Press MF, Rampersaud E, Rasmussen-Torvik LJ, Rodriguez-Gil JL, Salako B, Schadt EE, Schwartz
856 AG, Shriner DA, Siscovick D, Smith SB, Wassertheil-Smoller S, Speliotes EK, Spitz MR, Sucheston L,
857 Taylor H, Tayo BO, Tucker MA, Van Den Berg DJ, Edwards DR, Wang Z, Wiencke JK, Winkler TW,
858 Witte JS, Wrensch M, Wu X, Yang JJ, Levin AM, Young TR, Zakai NA, Cushman M, Zanetti KA, Zhao
859 JH, Zhao W, Zheng Y, Zhou J, Ziegler RG, Zmuda JM, Fernandes JK, Gilkeson GS, Kamen DL, Hunt
860 KJ, Spruill IJ, Ambrosone CB, Ambs S, Arnett DK, Atwood L, Becker DM, Berndt SI, Bernstein L, Blot
861 WJ, Borecki IB, Bottinger EP, Bowden DW, Burke G, Chanock SJ, Cooper RS, Ding J, Duggan D,
862 Evans MK, Fox C, Garvey WT, Bradfield JP, Hakonarson H, Grant SF, Hsing A, Chu L, Hu JJ, Huo D,
863 Ingles SA, John EM, Jordan JM, Kabagambe EK, Kardia SL, Kittles RA, Goodman PJ, Klein EA,
864 Kolonel LN, Le Marchand L, Liu S, McKnight B, Millikan RC, Mosley TH, Padhukasahasram B, Williams
865 LK, Patel SR, Peters U, Pettaway CA, Peyser PA, Psaty BM, Redline S, Rotimi CN, Rybicki BA, Sale
866 MM, Schreiner PJ, Signorello LB, Singleton AB, Stanford JL, Strom SS, Thun MJ, Vitolins M, Zheng W,
867 Moore JH, Williams SM, Ketkar S, Zhu X, Zonderman AB; NABEC Consortium; UKBEC Consortium;
868 BioBank Japan Project; AGEN Consortium; Kooperberg C, Papanicolaou GJ, Henderson BE, Reiner
869 AP, Hirschhorn JN, Loos RJ, North KE, Haiman CA. A meta-analysis identifies new loci associated with
870 body mass index in individuals of African ancestry. *Nat Genet.* 2013 Jun;45(6):690-6. doi:
871 10.1038/ng.2608. Epub 2013
872

873 Voss U, Sand C, Pfeiffer AF. Heterogeneity of insulin responses: phases leading to type 2 diabetes.
874 *PLoS One.* 2012;7(9):e44134. doi:10.1371/journal.pone.0044134
875

876 Remedi MS, Nichols CG. Hyperinsulinism and diabetes: genetic dissection of beta cell metabolism-
877 expectations and surprises. *Annu Rev Physiol.* 2009;71:647-662. doi:10.1146/
878 annurev.physiol.010908.163135
879

880 Milenkovic D, Sanz-Moreno A, Calzada-Wack J, Rathkolb B, Veronica Amarie O, Gerlini R, Aguilar-
881 Pimentel A, Misic J, Simard ML, Wolf E, Fuchs H, Gailus-Durner V, de Angelis MH, Larsson NG. Mice
882 lacking the mitochondrial exonuclease MGME1 develop inflammatory kidney disease with glomerular
883 dysfunction. *PLoS Genet.* 2022 May 9;18(5):e1010190
884

885 Robichon C, Varret M, Le Liepvre X, Lasnier F, Hajduch E, Ferré P, Dugail I. DnaJA4 is a SREBP-
886 regulated chaperone involved in the cholesterol biosynthesis pathway. *Biochim Biophys Acta.* 2006
887 Sep;1761(9):1107-13. doi: 10.1016/j.bbaliip.2006.07.007.
888

889 Bai Z, Chai XR, Yoon MJ, Kim HJ, Lo KA, Zhang ZC, et al. Dynamic transcriptome changes during
890 adipose tissue energy expenditure reveal critical roles for long noncoding RNA regulators. *PLoS Biol.*
891 (2017) 15:e2002176. doi: 10.1371/journal.pbio.2002176
892

893 Chimienti F, Devergnas S, Pattou F, Schuit F, Garcia-Cuenca R, Vandewalle B, et al. (2006). In vivo
894 expression and functional characterization of the zinc transporter ZnT8 in glucose-induced insulin
895 secretion. *Journal of Cell Science*, 119(20), 4199-4206.
896

897 Sladek R, Rocheleau G, Rung J, Dina C, Shen L, Serre D, et al. (2007). A genome-wide association
898 study identifies novel risk loci for type 2 diabetes. *Nature*, 445(7130), 881-885.
899

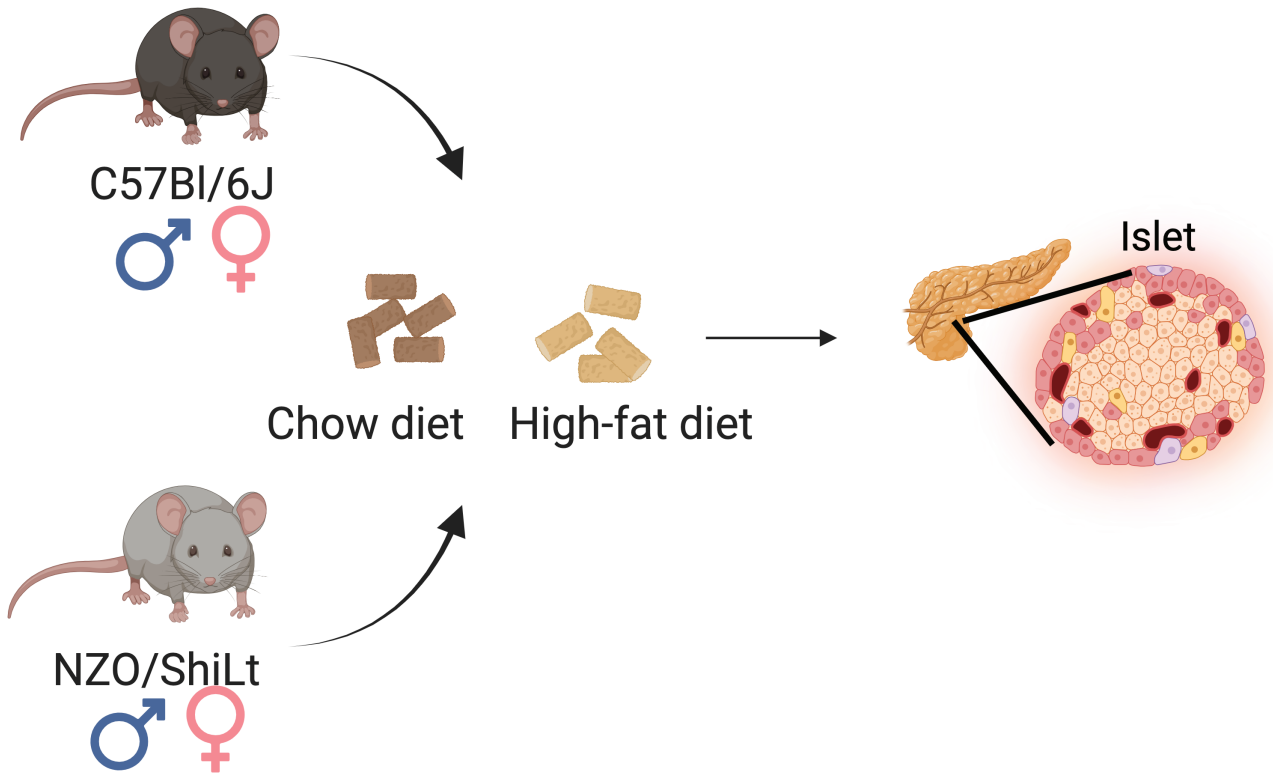
900 Scott LJ, Mohlke KL, Bonnycastle LL, Willer CJ, Li Y, Duren WL, et al. (2007). A genome-wide
901 association study of type 2 diabetes in Finns detects multiple susceptibility variants. *Science*,
902 316(5829), 1341-1345.
903

- 904 Mahajan et al. (2021). Refining the accuracy of validated target identification through coding variant
905 fine-mapping in type 2 diabetes. *Nature Genetics*, 53(10), 1380-1395
906
- 907 Gradwohl G, Dierich A, LeMeur M, Guillemot F. neurogenin3 is required for the development of the four
908 endocrine cell lineages of the pancreas. *Proc Natl Acad Sci U S A*. 2000 Feb 15;97(4):1607-11
909
- 910
- 911
- 912 Hrovatin, K., Bastidas-Ponce, A., Bakhti, M. et al. Delineating mouse β -cell identity during lifetime and
913 in diabetes with a single cell atlas. *Nat Metab* 5, 1615–1637 (2023)
914
- 915 Camunas-Soler J, Dai XQ, Hang Y, Bautista A, Lyon J, Suzuki K, Kim SK, Quake SR, MacDonald PE.
916 Patch-Seq Links Single-Cell Transcriptomes to Human Islet Dysfunction in Diabetes. *Cell Metab*. 2020
917 May 5;31(5):1017-1031.e4.
918
- 919 Bakhti, Mostafa, Anika Böttcher, and Heiko Lickert. Modelling the endocrine pancreas in health and
920 disease. *Nature Reviews Endocrinology* 15.3 (2019): 155-171.
921
- 922 Anna B. Osipovich, Jennifer S. Stancill, Jean-Philippe Cartailier, Karrie D. Dudek, Mark A. Magnuson;
923 Excitotoxicity and Overnutrition Additively Impair Metabolic Function and Identity of Pancreatic β -
924 Cells. *Diabetes* 1 July 2020; 69 (7): 1476–1491
925
- 926 Stancill JS, Cartailier JP, Clayton HW, O'Connor JT, Dickerson MT, Dadi PK, Osipovich AB, Jacobson
927 DA, Magnuson MA. Chronic β -Cell Depolarization Impairs β -Cell Identity by Disrupting a Network of
928 Ca²⁺-Regulated Genes. *Diabetes*. 2017 Aug;66(8):2175-2187.
929
- 930 Rudkowska I, Guénard F, Julien P, Couture P, Lemieux S, Barbier O, Calder PC, Minihane AM, Vohl
931 MC. Genome-wide association study of the plasma triglyceride response to an n-3 polyunsaturated
932 fatty acid supplementation. *J Lipid Res*. 2014 Jul;55(7):1245-53.
933
- 934 Franke A, Hampe J, Rosenstiel P, Becker C, Wagner F, Häslér R, Little RD, Huse K, Ruether A,
935 Balschun T, Wittig M, Elsharawy A, Mayr G, Albrecht M, Prescott NJ, Onnie CM, Fournier H, Keith T,
936 Radelof U, Platzer M, Mathew CG, Stoll M, Krawczak M, Nürnberg P, Schreiber S. Systematic
937 association mapping identifies NELL1 as a novel IBD disease gene. *PLoS One*. 2007 Aug 8;2(8):e691
938
- 939 Drucker DJ, Nauck MA. The incretin system: glucagon-like peptide-1 receptor agonists and dipeptidyl
940 peptidase-4 inhibitors in type 2 diabetes. *Lancet*. 2006 Nov 11;368(9548):1696-705.
941 Ussher, J.R., Drucker, D.J. Glucagon-like peptide 1 receptor agonists: cardiovascular benefits and
942 mechanisms of action. *Nat Rev Cardiol* 20, 463–474 (2023).
943
- 944 Müller TD, Finan B, Bloom SR, D'Alessio D, Drucker DJ, Flatt PR, Fritsche A, Gribble F, Grill HJ,
945 Habener JF, Holst JJ, Langhans W, Meier JJ, Nauck MA, Perez-Tilve D, Pocai A, Reimann F, Sandoval
946 DA, Schwartz TW, Seeley RJ, Stemmer K, Tang-Christensen M, Woods SC, DiMarchi RD, Tschöp MH.
947 Glucagon-like peptide 1 (GLP-1). *Mol Metab*. 2019 Dec;30:72-130.
948
- 949 Viana-Huete V, Guillen C, Garcia-Aguilar A, Garcia G, Fernandez S, Kahn CR, et al. Essential role of
950 IGFIR in the onset of Male brown fat thermogenic function: Regulation of glucose homeostasis by
951 differential organ-specific insulin sensitivity. *Endocrinology* (2016) 157(4):1495–511.
952

953 O'Neill BT, Lauritzen HP, Hirshman MF, Smyth G, Goodyear LJ, Kahn CR. Differential Role of
954 Insulin/IGF-1 Receptor Signaling in Muscle Growth and Glucose Homeostasis. *Cell Rep*. 2015 May
955 26;11(8):1220-35.
956
957 Nishimura W., Takahashi S., Yasuda K. MafA is critical for maintenance of the mature beta cell
958 phenotype in mice. *Diabetologia*. 2015;58:566–574.
959
960 Huang Q, Deng G, Wei R, Wang Q, Zou D, Wei J. Comprehensive Identification of Key Genes Involved
961 in Development of Diabetes Mellitus-Related Atherogenesis Using Weighted Gene Correlation Network
962 Analysis. *Front Cardiovasc Med*. 2020 Oct 28;7:580573.
963
964 Cromer MK, Choi M, Nelson-Williams C, Fonseca AL, Kunstman JW, Korah RM, Overton JD, Mane S,
965 Kenney B, Malchoff CD, Stalberg P, Akerström G, Westin G, Hellman P, Carling T, Björklund P, Lifton
966 RP. Neomorphic effects of recurrent somatic mutations in Yin Yang 1 in insulin-producing adenomas.
967 *Proc Natl Acad Sci U S A*. 2015 Mar 31;112(13):4062-7.
968
969 Dickinson, M. E., Flenniken, A. M., Ji, X., Teboul, L., Wong, M. D., White, J. K., Meehan, T. F.,
970 Weninger, W. J., Westerberg, H., & Adissu, H. (2016). High-throughput discovery of novel
971 developmental phenotypes. *Nature*, 537(7621), 508-514.
972
973 Groza, T., Gomez, F. L., Mashhadi, H. H., Muñoz-Fuentes, V., Gunes, O., Wilson, R., Cacheiro, P.,
974 Frost, A., Keskivali-Bond, P., & Vardal, B. (2023). The International Mouse Phenotyping Consortium:
975 comprehensive knockout phenotyping underpinning the study of human disease. *Nucleic acids*
976 *research*, 51(D1), D1038-D1045.
977
978 Kang, H. M., Subramaniam, M., Targ, S., Nguyen, M., Maliskova, L., McCarthy, E., Wan, E., Wong, S.,
979 Byrnes, L., & Lanata, C. M. (2018). Multiplexed droplet single-cell RNA-sequencing using natural
980 genetic variation. *Nature biotechnology*, 36(1), 89-94.
981
982 Keane, T. M., Goodstadt, L., Danecek, P., White, M. A., Wong, K., Yalcin, B., Heger, A., Agam, A.,
983 Slater, G., & Goodson, M. (2011). Mouse genomic variation and its effect on phenotypes and gene
984 regulation. *Nature*, 477(7364), 289-294.
985
986 Love, M. I., Huber, W., & Anders, S. (2014). Moderated estimation of fold change and dispersion for
987 RNA-seq data with DESeq2. *Genome Biology*, 15, 1-21.
988

Figure 1

A



B

Perturbed genes and their causal network.

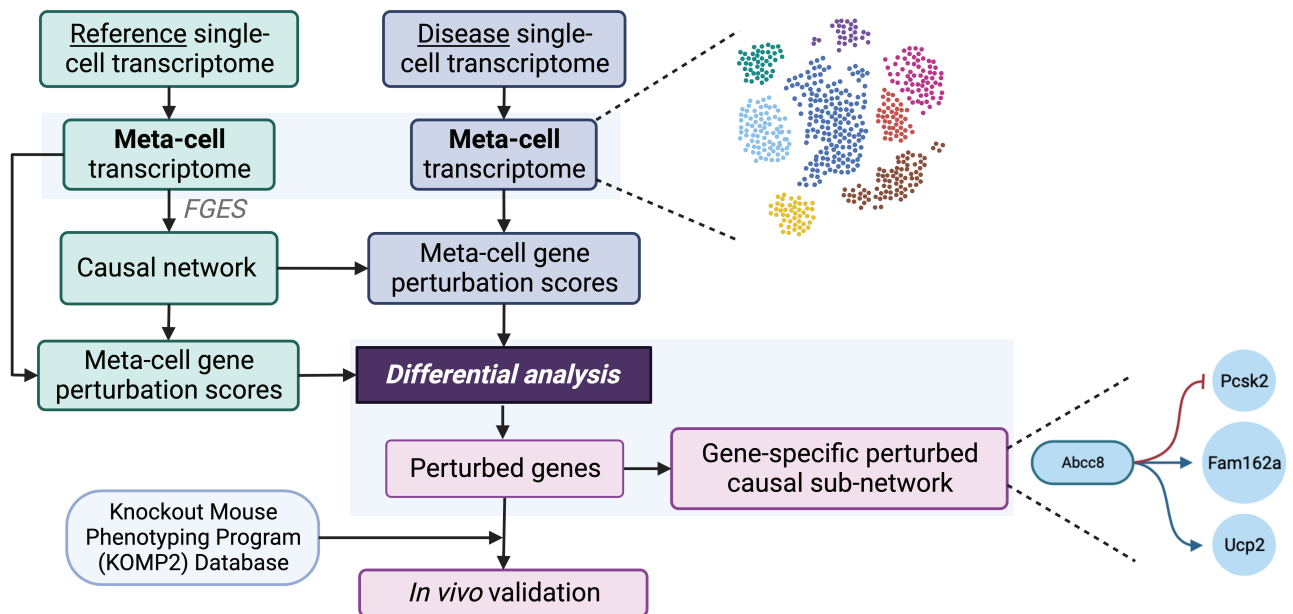
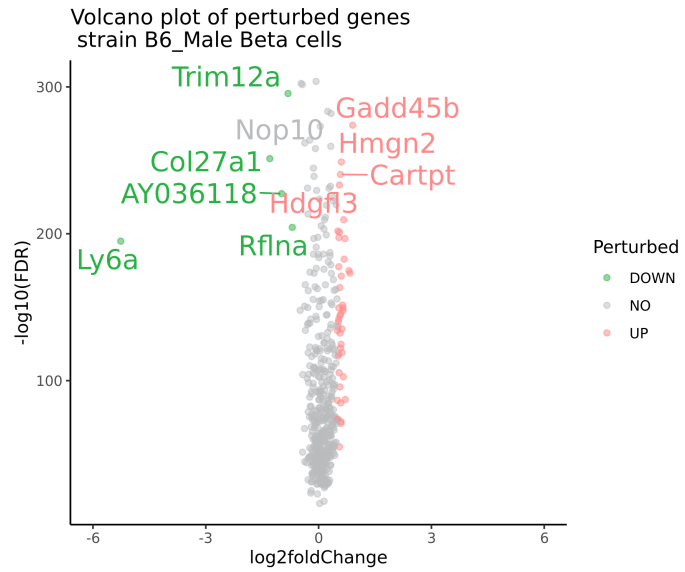
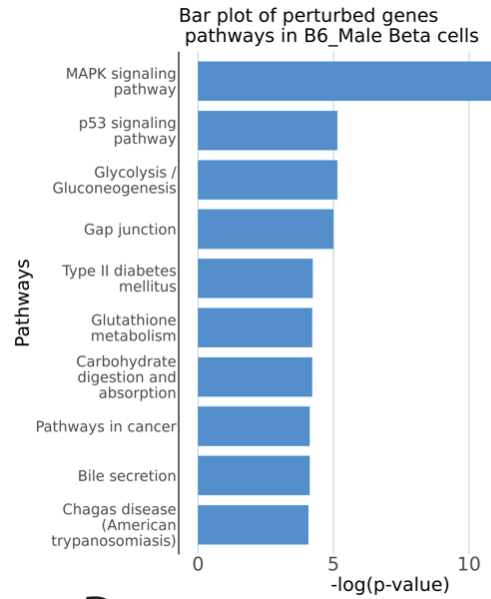


Figure 2: Identification of DEGs and perturbed genes from β -cells of C57BL/6J mice fed on a normal or high-fat high sugar diet

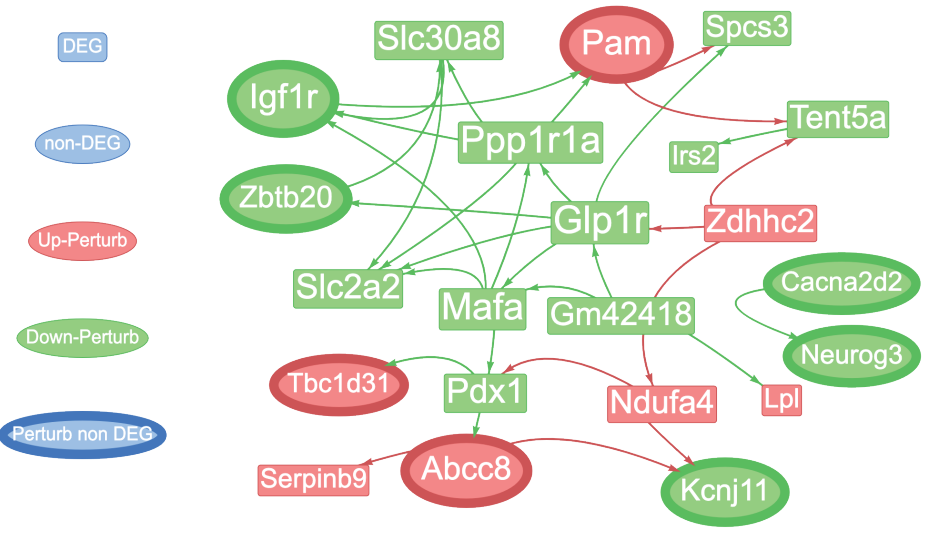
A



B



C



D

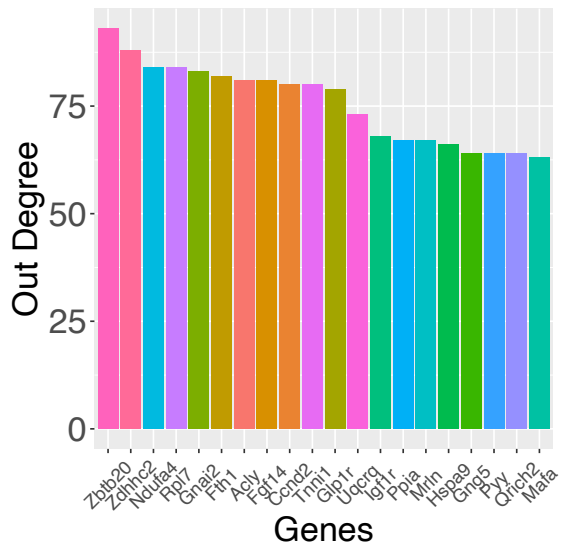


Figure 3: Identification of DEGs and perturbed genes from β -cells of C57BL/6J mice fed on a normal or high-fat high sugar diet KOMP validation

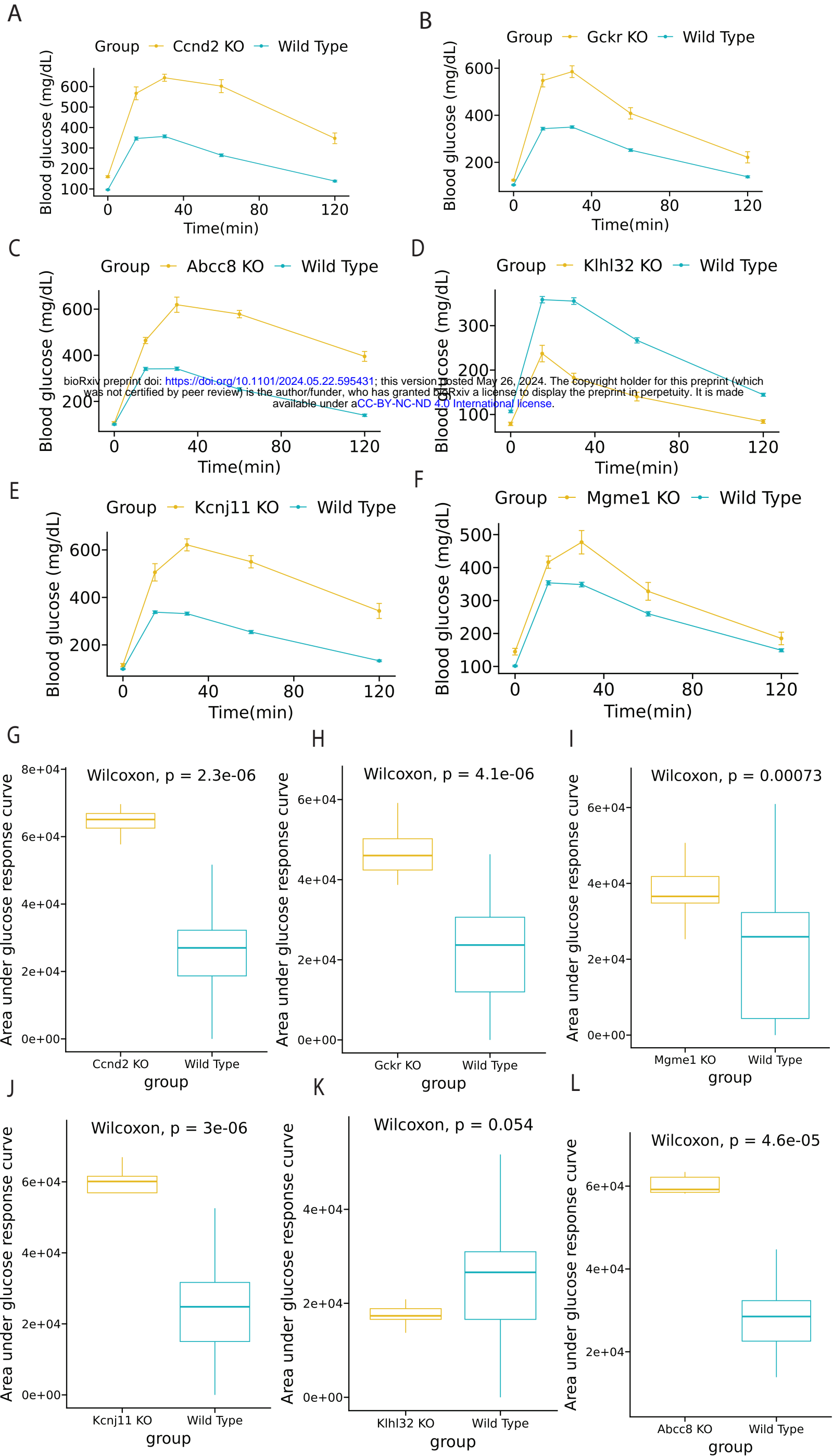


Figure 4: Identification of DEGs and perturbed genes from β -cells of NZO mice fed on a normal or high-fat high-sugar diet (Males)

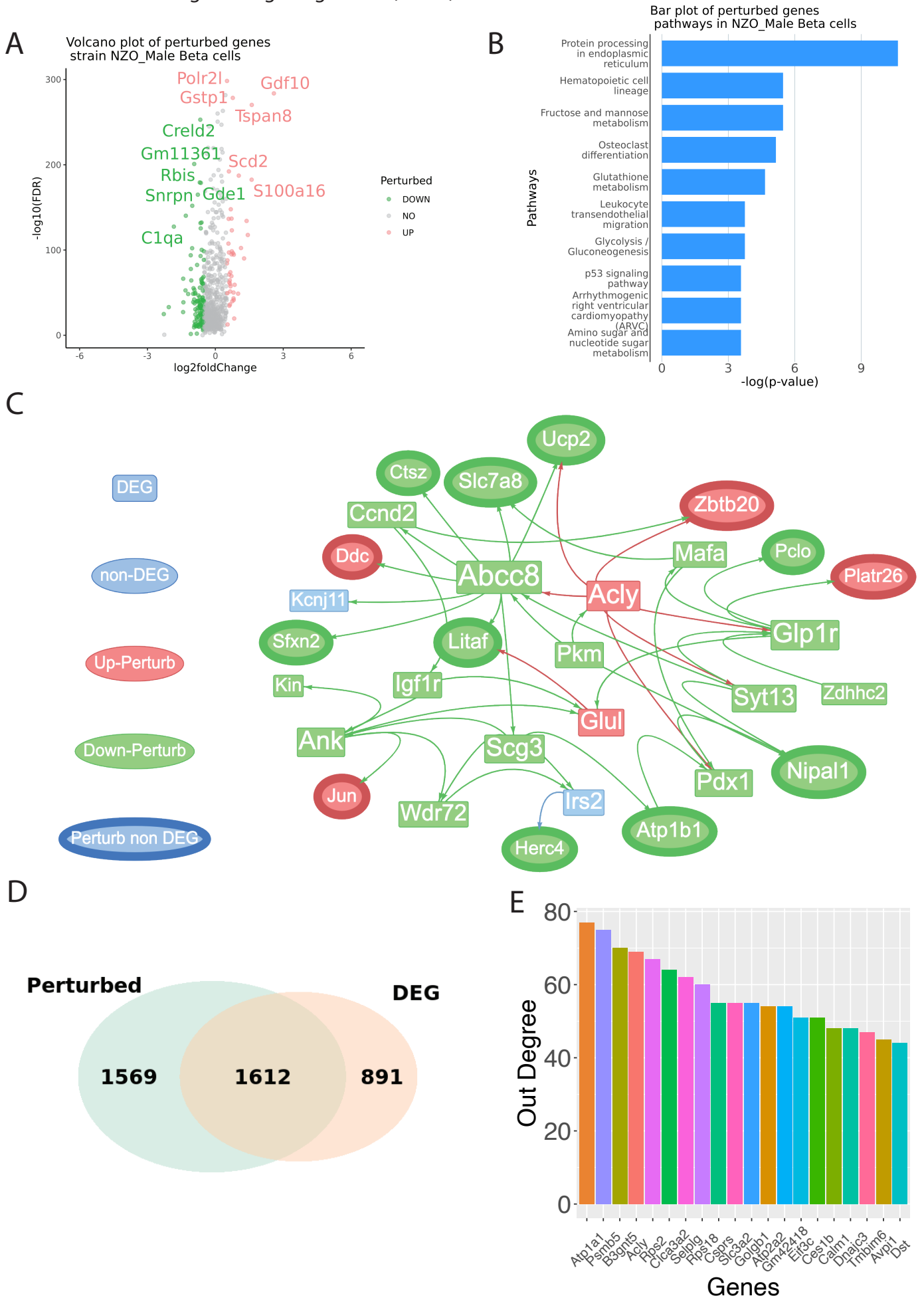


Figure 5: KOMP validation from β -cells of NZO mice fed on a normal or high-fat high-sugar diet (Males)

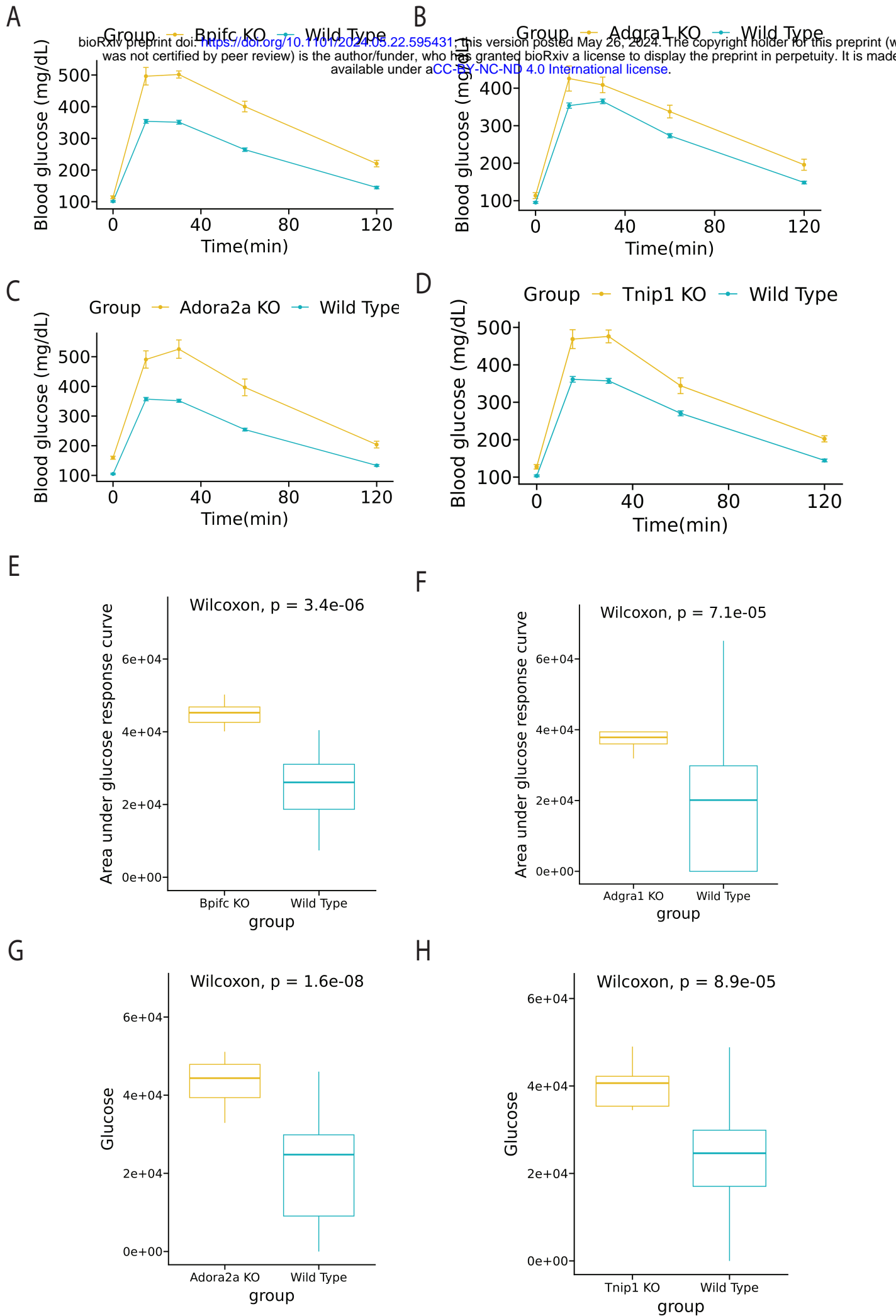


Figure 6: Identification of DEGs and perturbed genes from β -cells of C57BL/6J and NZO mice (males) fed on a high-fat high-sugar diet

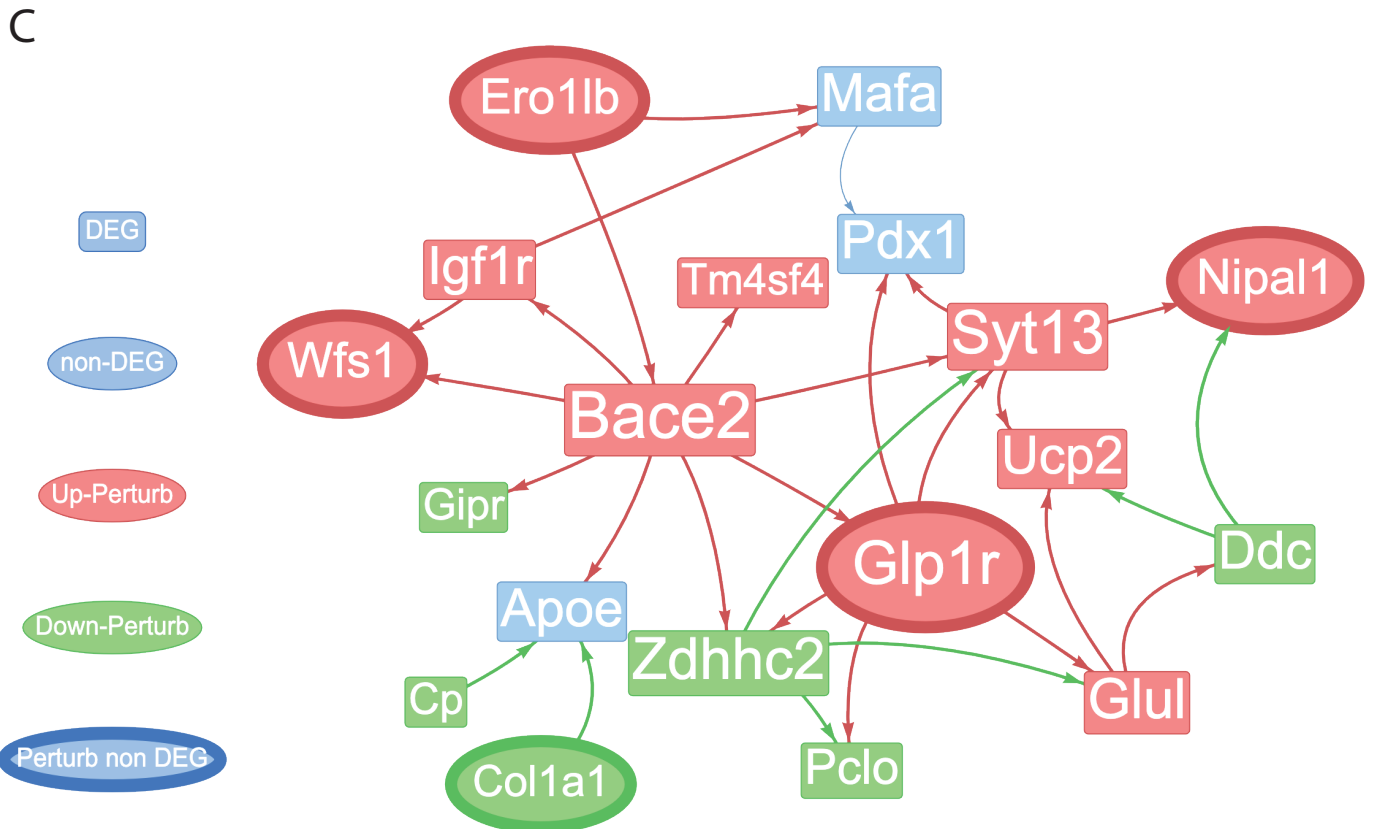
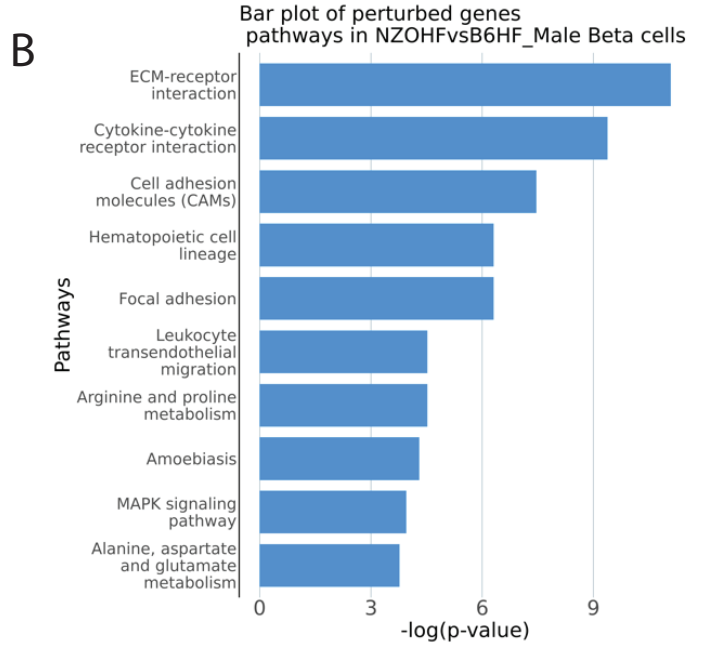
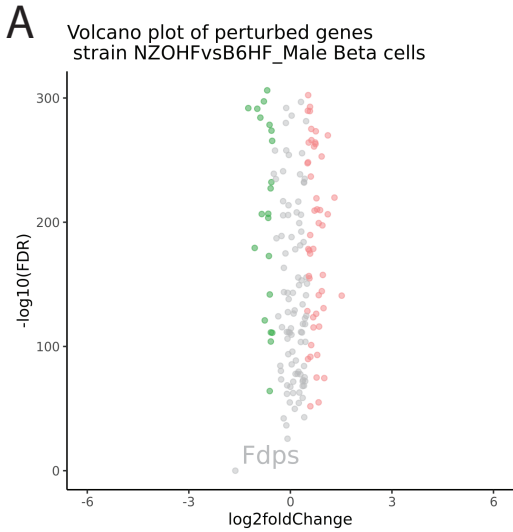


Figure 7: Identification of DEGs and perturbed genes from β -cells of C57BL/6J and NZO mice (males) fed on a high-fat high-sugar diet

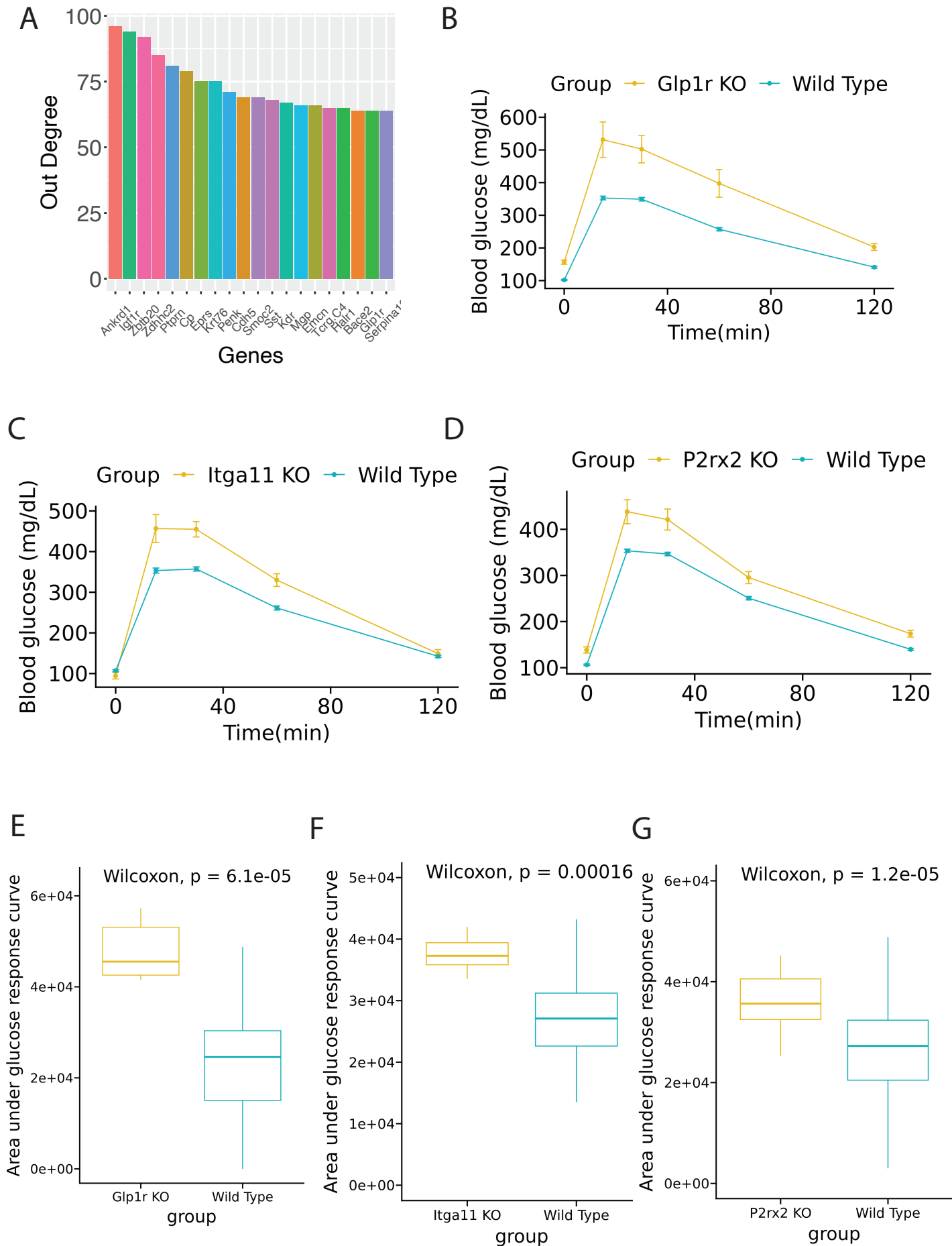
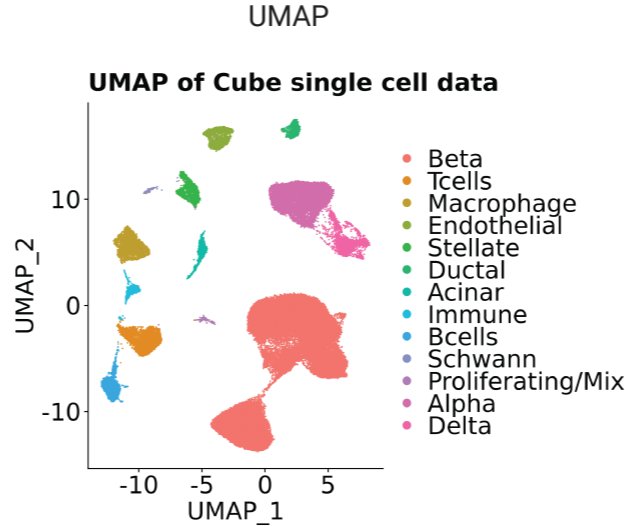
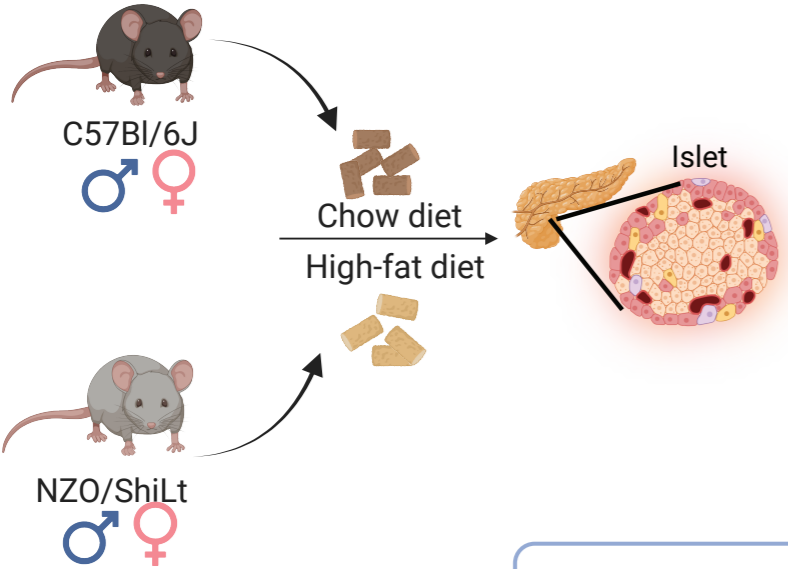
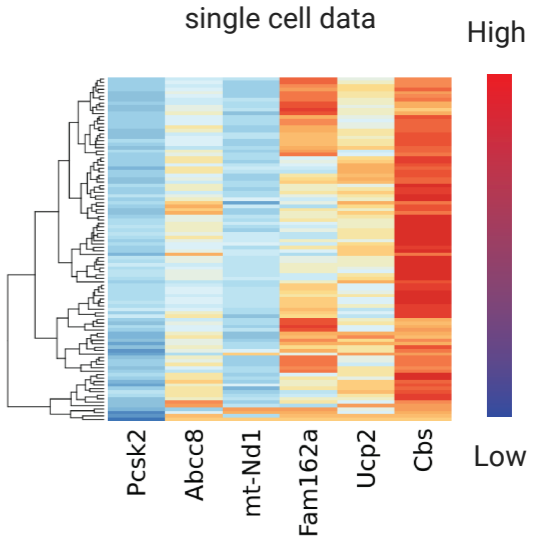


Figure S0: Workflow of meta-cell ssNPA analysis



For one selected strain and cell types



meta-cell samples

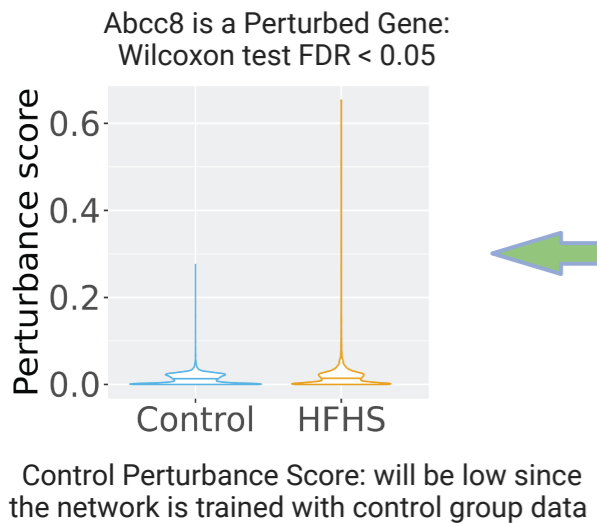
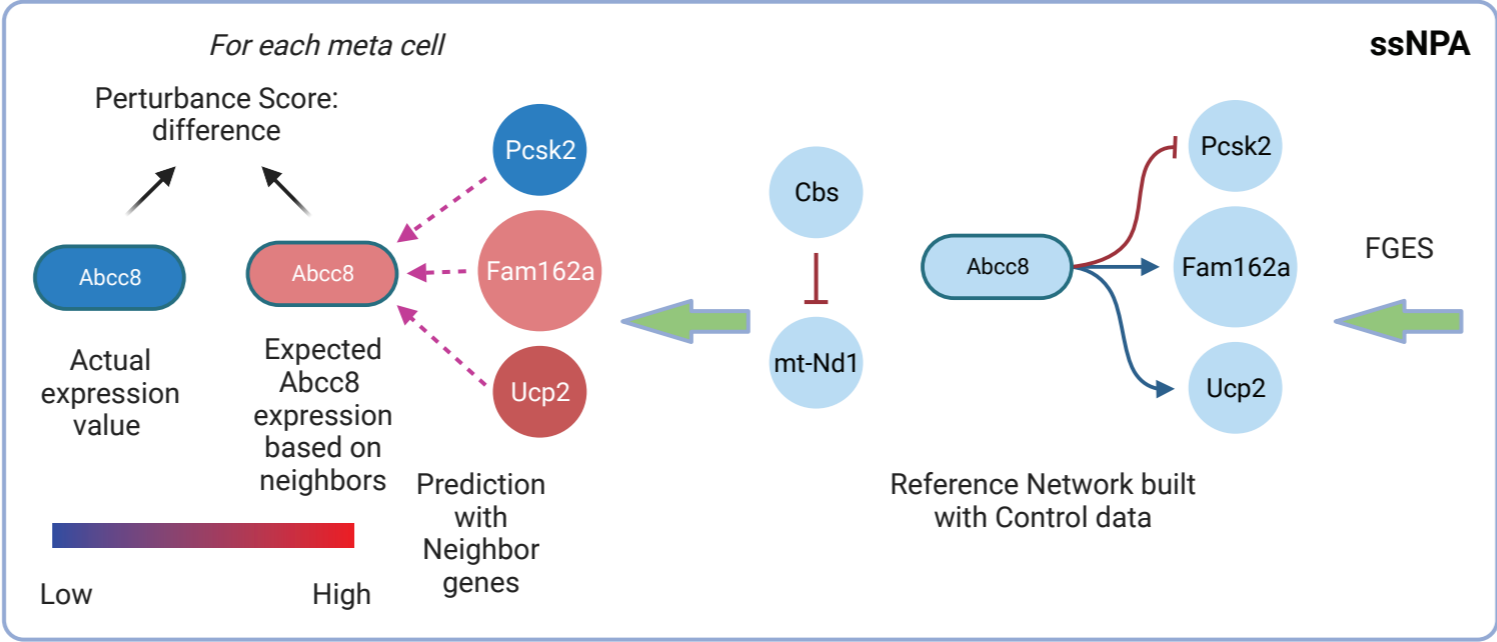
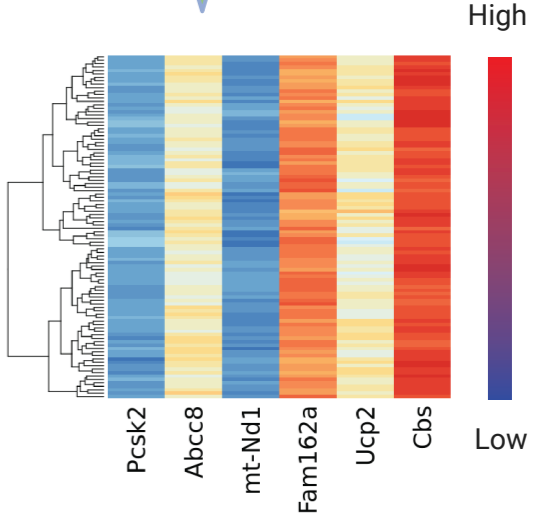
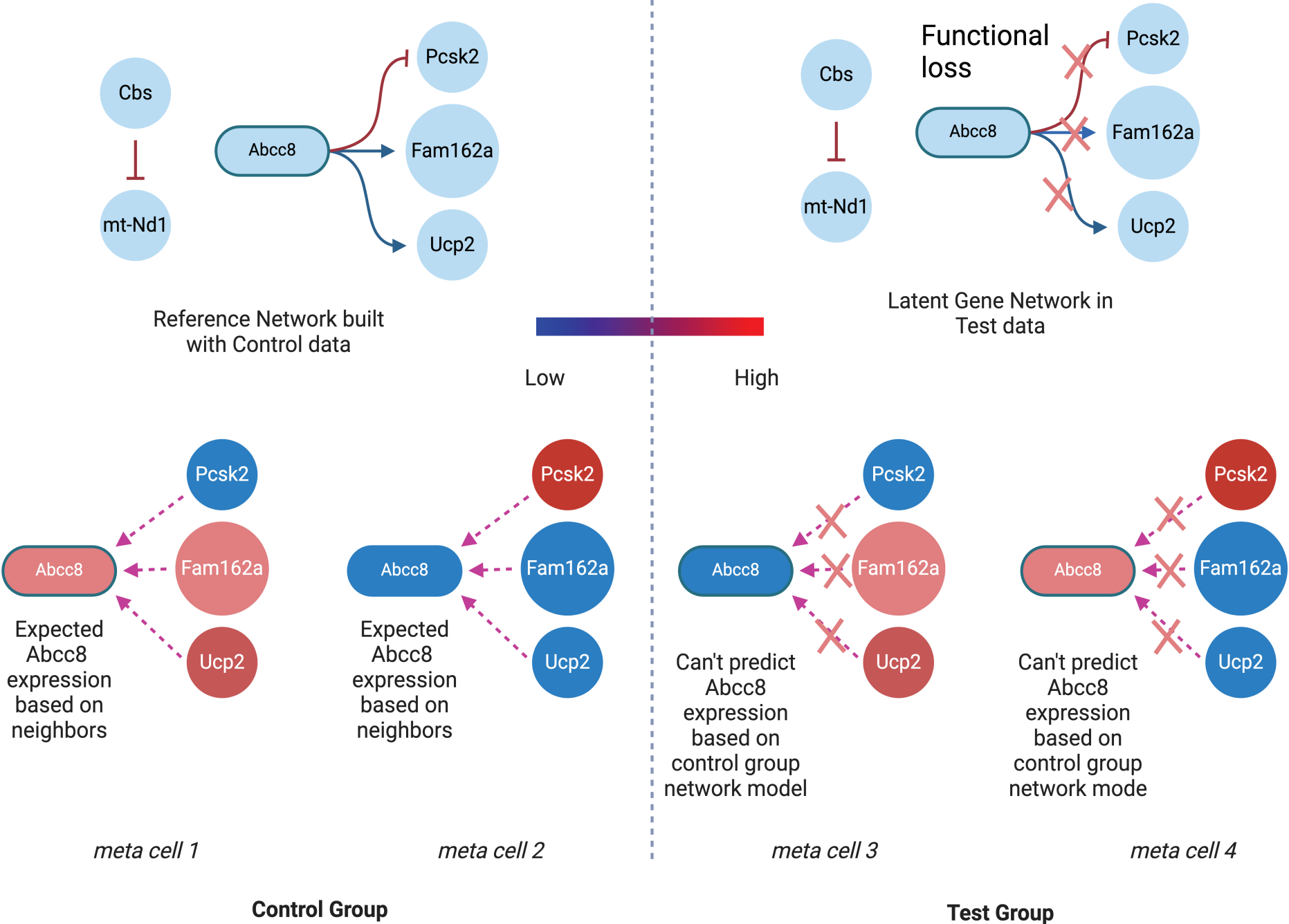


Figure S0': An example Abcc8 perturbation case where DEG analysis can't detect



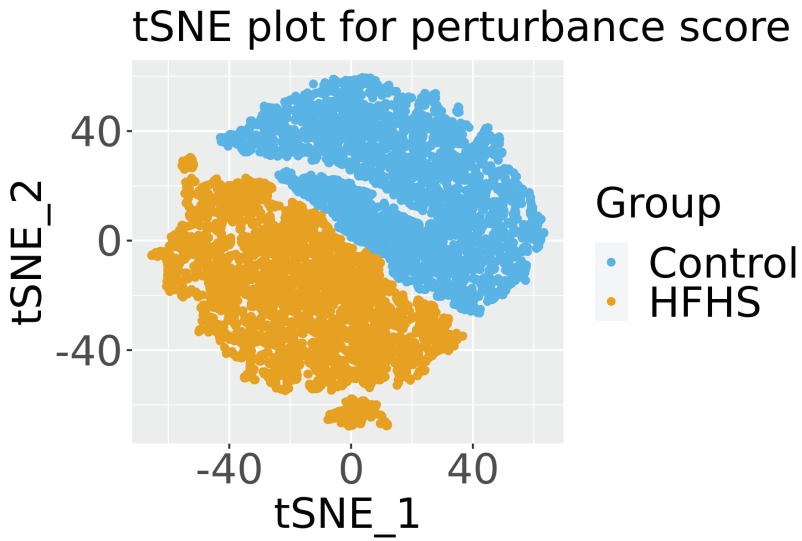
DEG analysis on Abcc8 between meta cell 1, meta cell 2 and meta cell 3, meta cell 4 will have p-value > 0.05

Figure S1: Full Network from β -cells of C57BL/6J mice fed on a normal or high-fat high-sugar diet

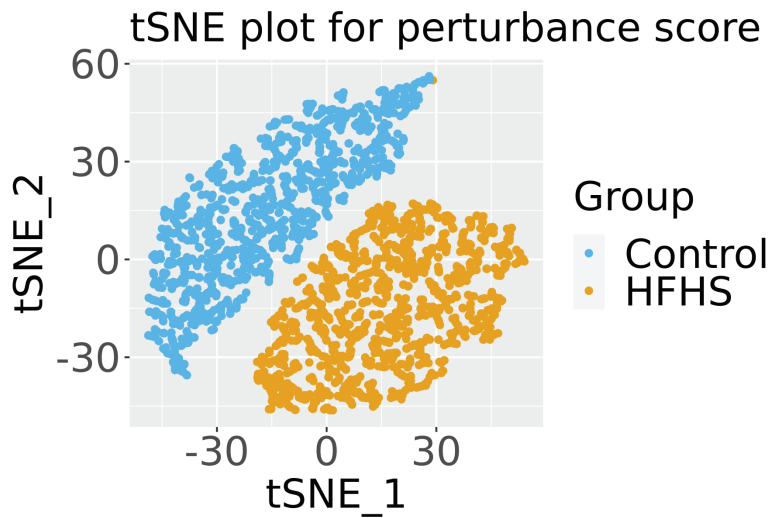


Figure S2: t-sne plots for petrubance score

B6 Male



NZO Male



NZO HF vs B6 HF Male

